Nonlinear optovibronics in molecular systems

Q. Zhang [1], M. Asjad [2], M. Reitz [3], C. Sommer [4], B. Gurlek [5] and C. Genes [1,6]

[1]*Max Planck Institute for the Science of Light, D-91058 Erlangen, Germany*
[2]*Department of Mathematics, Khalifa University, Abu Dhabi 127788, United Arab Emirates*
[3]*Department of Chemistry and Biochemistry, University of California San Diego, La Jolla, California 92093, USA*
[4]*Alpine Quantum Technologies GmbH, 6020 Innsbruck, Austria*
[5]*Max Planck Institute for the Structure and Dynamics of Matter and Center for Free-Electron Laser Science, 22761 Hamburg, Germany*
[6]*Department of Physics, Friedrich-Alexander-Universität Erlangen-Nürnberg, D-91058 Erlangen, Germany*

(Received 31 October 2023; accepted 22 January 2024; published 20 February 2024)

We analytically tackle optovibronic interactions in molecular systems driven by either classical or quantum light fields. In particular, we examine a simple model of molecules with two relevant electronic levels, characterized by potential landscapes with different positions of minima along the internuclear coordinates and of varying curvatures. Such systems exhibit an electron-vibron interaction, which can be composed of linear and quadratic terms in the vibrational displacement. By employing a combination of conditional displacement and squeezing operators, we present analytical expressions based on a quantum Langevin equations approach, to describe the emission and absorption spectra of such nonlinear molecular systems. Furthermore, we examine the imprint of the quadratic interactions onto the transmission properties of a cavity-molecule system within the collective strong-coupling regime of cavity quantum electrodynamics.

DOI: 10.1103/PhysRevA.109.023714

I. INTRODUCTION

Optovibrational interactions in molecular systems occur in an indirect fashion as light couples to electronic transitions, which are in turn coupled to the vibrations of nuclei [1–4]. A standard description of electron-vibron interactions, under the Born-Oppenheimer approximation, is given by the Holstein Hamiltonian [5,6], which is a spin-boson model linear in the vibrational displacement. Some analytical treatments based on quantum Langevin equations (QLEs) [7–12] have been shown to provide approximate analytical results for this model for a large number of vibrational modes and in the presence of fast vibrational relaxation typically occurring in both bulk [8,13] and solvent environments [14]. Similar methods have been used in cavity optomechanics [15,16], where cavity-confined quantum light modes are coupled to macroscopic oscillators via the radiation pressure Hamiltonian, to study the strong photon-phonon coupling regime [17,18].

Such theoretical treatments are based on a polaron transformation which allows for the diagonalization of the bare Holstein Hamiltonian [19]. This can be understood as a conditional displacement operation, where the electronic state dictates whether or not a displacement in the vibrational subspace should be performed. In consequence, when a photon excites an electronic transition between two copies of the same harmonic potential landscape slightly shifted [see Fig. 1(a)], the vibrational state is excited to a coherent state. The underlying assumption here is however that the potential landscapes are identical. In reality it can happen that the curvatures of the two potential-energy surfaces are different, as illustrated in Fig. 1(b): an electronic transition will then be accompanied by a squeezing of the vibrational wave packet. In such a case the polaron transformation is modified by an operation involving a conditional squeezing operator. Most generally, one can imagine the situation depicted in Fig. 1(c) where the proper diagonalizing transformation involves a conditional displacement followed by squeezing. In optomechanics, this corresponds to a quadratic photon-phonon interaction [20].

We provide here an analytical treatment based on a set of QLEs for effective spin operators dressed by vibrations, which can be solved under some approximations to provide information about emission and absorption spectra. Additionally, we investigate the transmission properties of an optical cavity within the strong-coupling regimes of cavity quantum electrodynamics. By studying the interaction between the molecular systems and the cavity, we gain insight into the nature of light-matter interactions in these complex environments.

The paper is organized as follows: in Sec. II we introduce the modified Holstein model obtained from first-principles derivations of the electron-vibration coupling for a scenario depicted in Fig. 1(c). Our analytical treatment is based on a set of simplified QLEs for vibrations and electronic degrees of freedom as derived in Sec. III. We proceed with solving the QLEs under the approximation of weak excitation of the upper electronic state to obtain absorption and emission spectra under illumination with classical light. Finally, in Sec. IV we add a quantum confined light field coupled to the electronic transition via the Tavis-Cummings Hamiltonian and derive the transmission profile of the cavity in the strong-coupling regimes of light-matter interactions.

Published by the American Physical Society under the terms of the Creative Commons Attribution 4.0 International license. Further distribution of this work must maintain attribution to the author(s) and the published article's title, journal citation, and DOI. Open access publication funded by the Max Planck Society.

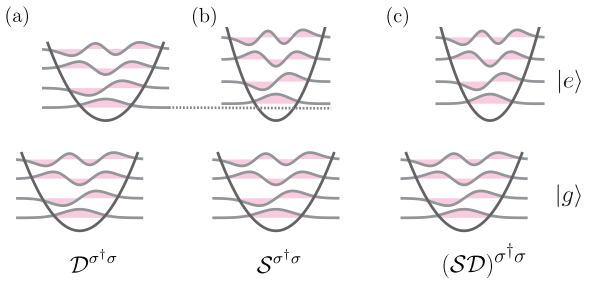

FIG. 1. (a) Standard scenario where the excited-state potential landscape is a copy of the ground-state landscape slightly shifted. Electronic excitation is accompanied by the action of a conditional displacement operator $\mathcal{D}^{\sigma^\dagger\sigma}$, where σ is the ladder operator from the excited to the ground electronic state. (b) Scenario with unshifted potentials with different curvatures. Electronic excitation is accompanied by a conditional squeezing operation $\mathcal{S}^{\sigma^\dagger\sigma}$. (c) Combined model where electronic excitation leads to a displacing and squeezing operation.

II. THE MODIFIED HOLSTEIN MODEL

We consider a molecule with two relevant electronic states denoted by $|g\rangle$ and $|e\rangle$ for ground and excited, respectively. Transitions between these two states are characterized by Pauli lowering operators $\sigma = |g\rangle\langle e|$ and their corresponding Hermitian conjugates. As illustrated in Fig. 1(c), the ground and excited potential landscapes are assumed to have a parabolic shape, with the minima of these two potential landscapes separated by R_{eg} and with different curvatures, thus having different vibrational frequencies: ν_g for the electronic ground state and ν_e for the electronic excited state. This is typically obtained as an approximation of Morse-type potential surfaces [21], as widely employed in theoretical studies [1,12,22,23]. In particular we refer to molecules in solid-state host matrices, where rotations are frozen and the fast vibrational relaxation ensures that states with more than one vibrational excitation are never reached, thus rendering anharmonic effects negligible. The Hamiltonian describing the molecular system can be expressed as ($\hbar = 1$)

$$\mathcal{H} = \mathcal{V}_e(\hat{R},\hat{P})\sigma^\dagger\sigma + \mathcal{V}_g(\hat{R},\hat{P})\sigma\sigma^\dagger, \tag{1}$$

where $\mathcal{V}_e$ and $\mathcal{V}_g$ denote the potential landscapes in the electronic excited and ground state, respectively, defined onto the direction of the nuclear coordinate as

$$\mathcal{V}_e(\hat{R},\hat{P}) = \omega_e + \frac{\hat{P}^2}{2\mu} + \frac{1}{2}\mu\nu_e^2(\hat{R}-R_{eg})^2, \tag{2a}$$

$$\mathcal{V}_g(\hat{R},\hat{P}) = \omega_g + \frac{\hat{P}^2}{2\mu} + \frac{1}{2}\mu\nu_g^2\hat{R}^2, \tag{2b}$$

with the reduced mass μ, and the momentum and position operators $\hat{P}$ and $\hat{R}$ satisfying the commutation relation $[\hat{R},\hat{P}] = i$. Notice that the matrix elements of the Hamiltonian $\mathcal{H}$ can be written in a basis formed by $\{|g;m_g\rangle = |g\rangle\otimes|m_g\rangle\,, |e;m_e\rangle = |e\rangle\otimes|m_e\rangle\}$, where the Fock states $|m_e\rangle$ and $|m_g\rangle$, respectively, refer to the eigenstates of the vibrational Hamiltonian part contained in $\mathcal{V}_g(\hat{R},\hat{P})$ and $\mathcal{V}_e(\hat{R},\hat{P})$, respectively.

However, one can express the quadratures in terms of creation $b^\dagger = (\hat{R}/R_{\rm ZPM} - iR_{\rm ZPM}\hat{P})/\sqrt{2}$ and annihilation $b = (\hat{R}/R_{\rm ZPM} + iR_{\rm ZPM}\hat{P})/\sqrt{2}$ operators. The operators fulfill the following commutation $[b,b^\dagger] = 1$ and the zero-point motion is defined as $R_{\rm ZPM} = 1/\sqrt{2\mu\nu_g}$. Notice that the definition of this bosonic operator is performed with respect to the ground state such that it diagonalizes the ground-state vibrational problem. The Hamiltonian in Eq. (1) can now be written as

$$\mathcal{H} = \nu_g b^\dagger b + \omega_0\sigma^\dagger\sigma + \lambda_1\nu_g(b+b^\dagger)\sigma^\dagger\sigma + \lambda_2\nu_g(b+b^\dagger)^2\sigma^\dagger\sigma. \tag{3}$$

The linear coupling parameter results from the mismatch in the positions of the minima $\lambda_1 = -\mu\nu_e^2 R_{eg}R_{\rm ZPM}/\nu_g$ while the quadratic coupling parameter is proportional to the relative change in vibrational frequencies $\lambda_2 = (\nu_e^2-\nu_g^2)/(4\nu_g^2)$. The bare electronic frequency splitting is modified by the vibronic coupling $\omega_0 = \omega_e - \omega_g + \lambda_1^2\nu_g^3/\nu_e^2$. However, it is more convenient to use a single basis formulation where only the eigenstates of the harmonic oscillator in the ground state are considered, i.e., the eigenstates of $\nu_g b^\dagger b$ denoted by $\{|m_g\rangle\}$. To this end, one can take the level-dependent unitary transformation $\tilde{\mathcal{H}} = \mathcal{U}^\dagger\mathcal{H}\mathcal{U}$ with

$$\mathcal{U} = \mathcal{D}(r_d)^{\sigma^\dagger\sigma}\mathcal{S}(r_s)^{\sigma^\dagger\sigma} = \sigma\sigma^\dagger + \mathcal{D}(r_d)\mathcal{S}(r_s)\sigma^\dagger\sigma. \tag{4}$$

The definitions of the displacement and squeezing operators are the standard ones employed in quantum optics

$$\mathcal{D}(r_d) = e^{r_d(b^\dagger - b)} \quad \text{and} \quad \mathcal{S}(r_s) = e^{\frac{1}{2}r_s(b^2 - b^{\dagger 2})} \tag{5}$$

which employ the following displacement r_d and squeezing r_s parameters defined as

$$r_d = -\lambda_1\frac{\nu_g^2}{\nu_e^2} \quad \text{and} \quad r_s = \frac{1}{2}(\ln\nu_e - \ln\nu_g). \tag{6}$$

Finally, the Hamiltonian is expressed in diagonal form:

$$\tilde{\mathcal{H}} = \nu_g b^\dagger b\sigma\sigma^\dagger + (\nu_e b^\dagger b + \omega_{00})\sigma^\dagger\sigma, \tag{7}$$

where the effective frequency $\omega_{00} = \omega_e - \omega_g + (\nu_e - \nu_g)/2$ relates to the zero-phonon line.

This is nothing more than a generalized polaron transformation where the electronic coherence operator σ is *dressed* by the vibrational modes as $\sigma\mathcal{D}(r_d)\mathcal{S}(r_s)$ via both a displacement and a squeezing operation. This offers a recipe to obtain the intensity of vibronic transitions in the emission and absorption processes. Assuming the molecule initially in the excited state with zero vibrations $|e;0_e\rangle$, the probability of ending up in the state $|g;m_g\rangle$ is governed by the overlap between the two vibrational wave functions [see Fig. 2(a)] as

$$S_m^{\rm em} = |\langle m_g|0_e\rangle|^2 = |\langle m_g|\mathcal{S}(r_s)\mathcal{D}(r_d)|0_g\rangle|^2 = \frac{e^{-r_d^2\alpha}}{\cosh(r_s)}\left[H_m\left(\frac{\alpha r_d}{2\sqrt{\beta}}\right)\right]^2\frac{\beta^m}{m!}, \tag{8}$$

where $H_m(x)$ are Hermite polynomials, $\alpha = \tanh r_s + 1$, and $\beta = (\tanh r_s)/2$. Similarly, we can find the absorption probability amplitude for the absorption transition $|g;0_g\rangle \to |e;m_e\rangle$ via the Hermitian adjoint operator $\sigma^\dagger\mathcal{S}^\dagger(r_s)\mathcal{D}^\dagger(r_d)$ such that

$$S_m^{\rm ab} = \frac{e^{\alpha' r_d^2\exp(2r_s)}}{\cosh(r_s)}\left[H_m\left(-\frac{i\alpha' r_d e^{r_s}}{2\sqrt{\beta}}\right)\right]^2\frac{(-\beta)^m}{m!}, \tag{9}$$

with $\alpha' = \tanh r_s - 1$.

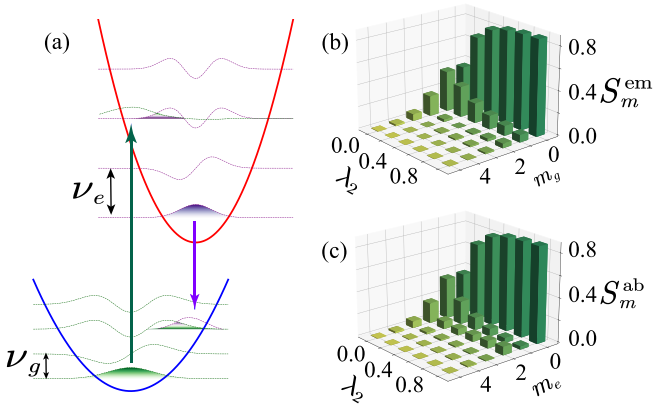

FIG. 2. (a) Schematic diagram of a molecular system exhibiting two parabolic electronic potential surfaces, slightly shifted and with different curvatures quantified by the vibrational frequencies ν_g and ν_e. Histogram of the vibrational state occupancy in the electronic ground state upon emission from $|e, 0_e\rangle$ in (b) and in the electronic excited state upon external drive from the $|g; 0_g\rangle$ state in (c) for various values of λ_2 at fixed $\lambda_1 = 1$.

We numerically illustrate the departure from such a statistics with various values of λ_2 in Figs. 2(b) and 2(c). Given the commutator $[\mathcal{D}(r_s), \mathcal{S}(r_s)] \neq 0$, the presence of the product $\mathcal{D}(r_s)\mathcal{S}(r_s)$ renders an asymmetry between the emission event $|e; 0_e\rangle \to |g; m_g\rangle$ and the absorption event $|g; 0_g\rangle \to |e; m_e\rangle$. Also, as a simple check, in the limiting case where $\lambda_2 = 0$, i.e., $\nu_e = \nu_g$, both transition strengths follow the same Poissonian distribution $\exp[-\lambda_1^2]\lambda_1^{2m}/m!$, as expected, reproducing the mirroring effect of emission and absorption spectra usually exhibited by most molecular transitions.

III. ABSORPTION AND EMISSION SPECTRA

In order to derive spectroscopic quantities, we will assume a continuous wave classical drive coupled to the electronic transition incorporated in the following Hamiltonian:

$$\mathcal{H}_\ell = i\eta_\ell(\sigma^\dagger e^{-i\omega_\ell t} - \sigma e^{i\omega_\ell t}), \tag{10}$$

with the Rabi frequency η_ℓ and laser frequency ω_ℓ. Since the molecule is also coupled to the electromagnetic vacuum and additional vibrational relaxation baths, we will make use of open system dynamics methods, first formulated in terms of a master equation. First, we include a spontaneous emission channel with the collapse operator σ at rate γ. In addition, as the electronic transition is modified by the vibrational mode [24–26], the influence of the environment onto the dynamics of the vibrational mode can be well described by a collapse operator $\mathcal{U}b\mathcal{U}^\dagger$ at the rate Γ. For numerical investigations, the master equation for the system is given:

$$\dot\rho = -i[\mathcal{H} + \mathcal{H}_\ell, \rho] + \mathcal{L}_\gamma[\sigma]\rho + \mathcal{L}_\Gamma[\mathcal{U}b\mathcal{U}^\dagger]\rho, \tag{11}$$

where the standard Lindblad superoperator is written as $\mathcal{L}_{\mathcal{O}}\cdot = \gamma_{\mathcal{O}}(2\mathcal{O}\cdot\mathcal{O}^\dagger - \mathcal{O}^\dagger\mathcal{O}\cdot - \cdot\mathcal{O}^\dagger\mathcal{O})$ for a collapse operator $\mathcal{O}$ and a corresponding decay rate $\gamma_{\mathcal{O}}$. In particular in the polaron transformation $\tilde\rho = \mathcal{U}^\dagger\rho\mathcal{U}$, the last term in Eq. (11) is going to the familiar form $\mathcal{L}_\Gamma[b]\tilde\rho$. The dot stands for the position where the density operator, on which the Lindblad superoperator is applied, is to be included.

It is convenient, for deriving analytical results, to map the master equation into an equivalent set of QLEs. For any system operator $\mathcal{A}$ this can be done as follows [7,27]:

$$\begin{aligned}\dot{\mathcal{A}} = &-i[\mathcal{A}, \mathcal{H} + \mathcal{H}_\ell] - [\mathcal{A}, \mathcal{O}^\dagger](\gamma_{\mathcal{O}}\mathcal{O} - \sqrt{2\gamma_{\mathcal{O}}}\mathcal{O}_{\rm in}) \\ &+ (\gamma_{\mathcal{O}}\mathcal{O}^\dagger - \sqrt{2\gamma_{\mathcal{O}}}\mathcal{O}_{\rm in}^\dagger)[\mathcal{A}, \mathcal{O}],\end{aligned} \tag{12}$$

where $\mathcal{O}_{\rm in}$ is the zero-averaged and delta-correlated input noise operator associated with the collapse operator $\mathcal{O}$ and $\gamma_{\mathcal{O}}$ is the associated decay rate.

For molecules in solid-state environments, the vibrational relaxation rate is usually very large, greatly surpassing both γ and η_ℓ. Therefore, fluorescence occurs preferentially from the state $|e, 0_e\rangle$, which lies at the bottom of the excited-state manifold: this is generally referred to as Kasha's rule [28]. The same mechanism is valid for the absorption process, where absorption occurs from the state $|g, 0_g\rangle$, the lowest in energy. We will make use of this fast vibrational relaxation to impose a quick timescale for the modification of the bosonic b operators and use their quasi-steady-state values in the following. First, however, let us partition the total Hilbert space into two orthogonal subspaces (ground and excited electronic state manifolds) via the following two projection operators: $\mathcal{P}_g = \sigma\sigma^\dagger$ and $\mathcal{P}_e = \sigma^\dagger\sigma$. Let us first pay attention to the dynamical equation in the manifold of $\mathcal{P}_e$. For convenience reasons, we introduce a projected bosonic operator $b_e = \mathcal{U}b\mathcal{U}^\dagger\mathcal{P}_e$ acting only in this manifold and more explicitly expressed as

$$b_e = (\cosh r_s b + \sinh r_s b^\dagger - r_d e^{r_s})\mathcal{P}_e \tag{13}$$

and obeying the relation $b_e^\dagger b_e\,|e; m_e\rangle = m_e\,|e; m_e\rangle$. Meanwhile, we define a time-dependent generalized polaron operator [7,8], by the transformation $\tilde\sigma_e = \sigma\mathcal{S}_e^\dagger\mathcal{D}_e^\dagger\exp[i(\nu_e - \nu_g)b_e^\dagger b_e t]$. This allows the derivation of a set of effective QLEs in the rotating frame at the driving frequency ω_ℓ for the emission process (see Appendix B for details):

$$\dot b_e \approx -(i\nu_e + \Gamma)b_e + \sqrt{2\Gamma}\mathcal{B}_e^{\rm in}\mathcal{P}_e, \tag{14a}$$

$$\begin{aligned}\dot{\tilde\sigma}_e \approx &-(i\Delta_\ell + \gamma)\tilde\sigma_e - \eta_\ell\mathcal{S}_e^\dagger\mathcal{D}_e^\dagger e^{i(\nu_e-\nu_g)b_e^\dagger b_e t} \\ &+ \sqrt{2\gamma}\sigma_{\rm in}\mathcal{S}_e^\dagger\mathcal{D}_e^\dagger e^{i(\nu_e-\nu_g)b_e^\dagger b_e t},\end{aligned} \tag{14b}$$

$$\dot{\mathcal{P}}_e = -2\gamma\mathcal{P}_e + \eta_\ell(\sigma + \sigma^\dagger) + \sqrt{2\gamma}(\sigma^\dagger\sigma_{\rm in} + \sigma_{\rm in}^\dagger\sigma), \tag{14c}$$

with the detuning $\Delta_\ell = \omega_{00} - \omega_\ell$, the displacement operator $\mathcal{D}_e = \exp[r_d(b_e^\dagger - b_e)]\mathcal{P}_e$, and the squeezing operator $\mathcal{S}_e = \exp[r_s(b_e^2 - b_e^{\dagger 2})/2]\mathcal{P}_e$. The input noises $\mathcal{B}_e^{\rm in}$ and $\sigma_{\rm in}$ are zero averaged and have the following two-time correlations: $\langle\mathcal{B}_e^{\rm in}(t)\mathcal{B}_e^{\rm in\dagger}(t')\rangle = \delta(t - t')$ and $\langle\sigma_{\rm in}(t)\sigma_{\rm in}^\dagger(t')\rangle = \delta(t - t')$.

In a very similar fashion, projected operators in the ground electronic state manifold can be defined. Let us introduce the ground-state polaron operator via the transformation $\tilde\sigma_g = \exp[i(\nu_e - \nu_g)b_g^\dagger b_g t]\mathcal{S}_g^\dagger\mathcal{D}_g^\dagger\sigma$ which allows one to derive

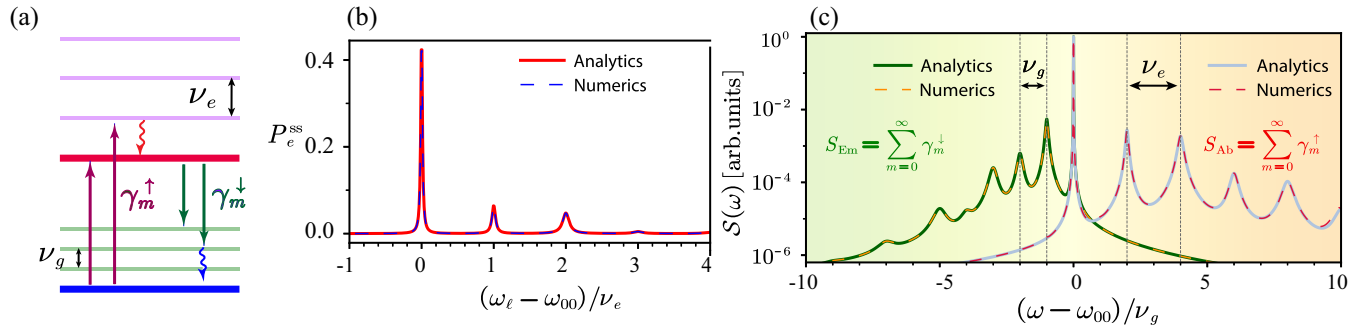

FIG. 3. (a) Jablonski diagram illustrating possible emission and absorption processes. (b) Comparison of analytical and numerical results of the excited-state population as a function of normalized detuning. Parameters are $\lambda_2 = 1$ (i.e., $\nu_e/\nu_g = 2$), $\Gamma/\nu_g = 0.1$, $\gamma/\Gamma = 0.1$, and $\eta_\ell/\gamma = 2$. (c) Comparison of analytical results vs numerical simulations for the absorption (shaded in orange) and emission (shaded in green) profiles. Parameters are $\eta_\ell/\gamma = 0.1$ and $\Delta_\ell/\nu_g = 0.1$.

a similar set of QLEs:

$$\dot{b}_g \approx -(i\nu_g + \Gamma)b_g + \sqrt{2\Gamma}\mathcal{B}_g^{\rm in}\mathcal{P}_g, \tag{15a}$$

$$\dot{\tilde{\sigma}}_g \approx -(i\Delta_\ell + \gamma)\tilde{\sigma}_g + \eta_\ell e^{i(\nu_e-\nu_g)b_g^\dagger b_g t}\mathcal{S}_g^\dagger\mathcal{D}_g^\dagger + \sqrt{2\gamma}e^{i(\nu_e-\nu_g)b_g^\dagger b_g t}\mathcal{S}_g^\dagger\mathcal{D}_g^\dagger\sigma_{\rm in}. \tag{15b}$$

As above, the new displacement operator is $\mathcal{D}_g = \exp[r_d(b_g^\dagger - b_g)]\mathcal{P}_g$, and the new squeezing operator is $\mathcal{S}_g = \exp[r_s(b_g^2 - b_g^{\dagger 2})/2]\mathcal{P}_g$. The nonvanishing correlation of the zero-average noise operator is given by $\langle\mathcal{B}_g^{\rm in}(t)\mathcal{B}_g^{\rm in\dagger}(t')\rangle = \delta(t-t')$.

We are now in the position of reconstructing the full solution of the coherence operator in steady state by summing over the contributions in the ground- and excited-state manifolds. This can be done by formal integration of Eqs. (14b) and (15b) to obtain a solution for $\langle\sigma\rangle$ expressed as

$$\langle\sigma\rangle = -\eta_\ell\int_0^\infty d\tau\,\Theta(t-\tau)e^{-(i\Delta_\ell+\gamma)(t-\tau)}\langle\mathcal{S}_e^\dagger(\tau)\mathcal{D}_e^\dagger(\tau)e^{i(\nu_e-\nu_g)b_e^\dagger b_e\tau}e^{-i(\nu_e-\nu_g)b_e^\dagger b_e t}\mathcal{D}_e(t)\mathcal{S}_e(t)\rangle + \eta_\ell\int_0^\infty d\tau\,\Theta(t-\tau)e^{-(i\Delta_\ell+\gamma)(t-\tau)}\langle\mathcal{D}_g(t)\mathcal{S}_g(t)e^{-i(\nu_e-\nu_g)b_g^\dagger b_g t}e^{i(\nu_e-\nu_g)b_g^\dagger b_g\tau}\mathcal{S}_g^\dagger(\tau)\mathcal{D}_g^\dagger(\tau)\rangle. \tag{16}$$

Here, we have used the Heaviside step function $\Theta(t)$ and the initial value $\langle\sigma(0)\rangle = 0$. Considering that the vibrational mode has a large relaxation rate (i.e., $\Gamma \gg \gamma$), we then decouple the vibronic and electronic degrees of freedom. The two-time correlation functions on the right side of the above equation can be expressed as (see Appendix B for details)

$$\langle\mathcal{D}_e(\tau)\mathcal{S}_e(\tau)e^{i(\nu_e-\nu_g)b_e^\dagger b_e\tau}e^{-i(\nu_e-\nu_g)b_e^\dagger b_e t}\mathcal{S}_e^\dagger(t)\mathcal{D}_e^\dagger(t)\rangle = \sum_{m=0}^\infty S_m^{\rm em}e^{-m(i\nu_g+\Gamma)(t-\tau)}\langle\mathcal{P}_e(\tau)\rangle, \tag{17a}$$

$$\langle\mathcal{D}_g(t)\mathcal{S}_g(t)e^{-i(\nu_e-\nu_g)b_g^\dagger b_g t}e^{i(\nu_e-\nu_g)b_g^\dagger b_g\tau}\mathcal{S}_g^\dagger(\tau)\mathcal{D}_g^\dagger(\tau)\rangle = \sum_{m=0}^\infty S_m^{\rm ab}e^{-m(-i\nu_e+\Gamma)(t-\tau)}\langle\mathcal{P}_g(\tau)\rangle. \tag{17b}$$

Replacing the infinite sums from above back into Eq. (16) leads to a convolution in time. This can be dealt with by employing a Laplace transformation defined as $\overline{f}(s) = \int_0^\infty dt\,f(t)\exp(-st)$ for a time-dependent function $f(t)$ at $t \geqslant 0$. In such a case, Eq. (16) takes a much simpler form

$$\overline{\langle\sigma\rangle} = \frac{\eta_\ell}{s}\overline{\mathcal{G}}_{\rm ab} - \eta_\ell\overline{\langle\mathcal{P}_e\rangle}(\overline{\mathcal{G}}_{\rm em} + \overline{\mathcal{G}}_{\rm ab}), \tag{18}$$

with the following functions identified corresponding to emission and absorption events, respectively:

$$\overline{\mathcal{G}}_{\rm em} = \sum_{m=0}^\infty \frac{S_m^{\rm em}}{s + m\Gamma + \gamma + i(\Delta_\ell - m\nu_g)}, \tag{19}$$

$$\overline{\mathcal{G}}_{\rm ab} = \sum_{m=0}^\infty \frac{S_m^{\rm ab}}{s + \gamma + m\Gamma + i(\Delta_\ell + m\nu_e)}. \tag{20}$$

From these expressions, one can proceed in evaluating analytically the population of the excited state $p_e^{\rm SS} = \lim_{t\to\infty}\langle\sigma^\dagger(t)\sigma(t)\rangle$ in steady state (as detailed in Appendix D):

$$p_e^{\rm SS} = \frac{\sum_{m=0}^\infty \gamma_m^{\uparrow}(\omega_\ell)}{\gamma + \sum_{m=0}^\infty[\gamma_m^{\uparrow}(\omega_\ell) + \gamma_m^{\downarrow}(\omega_\ell)]}. \tag{21}$$

The coefficients $\gamma_m^{\uparrow}(\omega)$ and $\gamma_m^{\downarrow}(\omega)$ represent the dynamic equilibrium population transfer rates for absorption from the ground state to the excited state $|g;0_g\rangle \to |e;m_e\rangle$ and emission from the excited to the ground state $|e;0_e\rangle \to |g;m_g\rangle$ as illustrated in Fig. 3(a). The rates are analytically expressed as

$$\gamma_m^{\uparrow}(\omega) = \frac{\eta_\ell^2 S_m^{\rm ab}(m\Gamma+\gamma)}{(m\Gamma+\gamma)^2 + (\omega_{00} + m\nu_e - \omega)^2}, \tag{22a}$$

$$\gamma_m^{\downarrow}(\omega) = \frac{\eta_\ell^2 S_m^{\rm em}(m\Gamma+\gamma)}{(m\Gamma+\gamma)^2 + (\omega_{00} - m\nu_g - \omega)^2}. \tag{22b}$$

Specifically, these rates contribute to the rate equation for the population of the excited state, given by (see Appendix E for detailed derivations)

$$\partial_t p_e = -2\left(\gamma + \sum_{m=0}^{\infty} \gamma_m^{\downarrow}\right) p_e + 2\sum_{m=0}^{\infty} \gamma_m^{\uparrow}(1 - p_e). \tag{23}$$

This equation holds true under the condition $\eta_\ell \ll \Gamma$. Remarkably, one can also obtain the same expression for the population of the excited state in steady state and compare it with full numerical simulations to a very good fit, as illustrated in Fig. 3(b). The parameters are given in the caption and are chosen in close attention to other works [29,30].

Additionally, we can employ the pump-probe scenario to analyze the absorption and emission processes. In this scenario, the molecule absorbs a photon at the frequency ω_ℓ, transitioning to the excited state $|e; m_e\rangle$ under the resonant condition $\omega_\ell = \omega_{00} + m v_e$. Subsequently, after undergoing fast vibrational relaxation, the molecule emits a photon centered around the frequency $\omega_{00} - m' v_g$, which can be detected with a modified linewidth $\gamma + m'\Gamma$. The absorption and emission profiles are then obtained by summing up the contributions from all possible cases, resulting in Lorentzian profiles represented by $\gamma_m^{\uparrow/\downarrow}$, as shown in Fig. 3(c):

$$S_{\rm ab} = \sum_{m=0}^{\infty} \gamma_m^{\uparrow} \quad \text{and} \quad S_{\rm em} = \sum_{m=0}^{\infty} \gamma_m^{\downarrow}. \tag{24}$$

Here, the scaling of the vibrational rates has been intentionally exaggerated in order to clearly point out the difference in energies expected for the smaller and higher-energy sidebands. The presence of the quadratic electron-vibron coupling under realistic conditions is expected to only slightly break the symmetry between the emission and absorption spectra, as the expected values for λ_2 lie well below in the subunit region. More details on the procedure we have followed for the above derivations are presented in Appendix F and basically follow the quantum regression theorem formalism [27,31].

IV. MOLECULAR POLARITONICS

Let us now ask what is the imprint of the asymmetry between the ground- and excited-state potential landscapes on the signal of an optical cavity containing such a molecule in the strong-coupling regime of cavity quantum electrodynamics. To this end, we consider a single molecule placed within the optical volume of a single mode optical cavity mediating transitions between the ground and excited potential landscapes. Under strong optical confinement conditions, the interaction of light and matter can lead to the production of hybrid quantum states, i.e., polaritons [1,12,23,32–38], as superpositions of ground or excited electronic states and zero- or single-photon states. While polaritons are eigenstates solely of the electron-photon interaction Hamiltonian, the intrinsic electron-vibron coupling can provide a mechanism of polariton cross talk, leading to a unidirectional loss of energy from the higher state to the lower-energy state. This has been shown analytically in Ref. [7] for the standard case of identical ground- and excited-state potential landscapes and found to be most pronounced when the vibrational mode is resonant to the interpolariton frequency splitting.

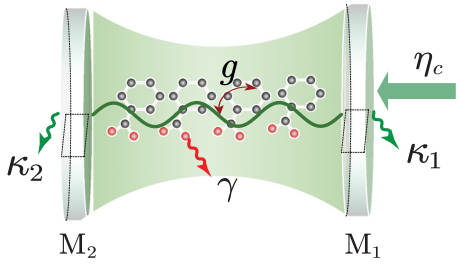

FIG. 4. Schematics of an ensemble of molecules inside a Fabry-Pérot resonator. Cavity photon loss occurs at rates κ_1 and κ_2 via the mirrors M1 and M2, respectively. Light-molecule interactions occur at rate g while spontaneous emission and cavity driving are at rates γ and η_c, respectively.

Let us now consider the case of $\mathcal{N}$ molecules inside the spatial extent of a single mode of a Fabry-Pérot optical resonator, as illustrated in Fig. 4. The dynamics of a single molecule is governed by the Hamiltonian $\mathcal{H}$ from Eq. (3). The interaction between the $\mathcal{N}$ molecules and the cavity field mode is characterized by the Tavis-Cummings model,

$$\mathcal{H}_{\rm cav} = \omega_c a^\dagger a + g\sum_{n=1}^{\mathcal{N}} (a\sigma_n^\dagger + \text{H.c.}) + i\eta_c(a^\dagger e^{-i\omega_\ell t} - \text{H.c.}), \tag{25}$$

consisting of the free cavity field at frequency ω_c and with bosonic mode a and the Tavis-Cummings interaction with the unit light-matter coupling strength g and the laser field drive with amplitude η_c and frequency ω_ℓ. For convenience, we have made the assumption here that all molecules are identical. Let us proceed with a set of effective QLEs for the cavity mode a and the state dependent polaron operators $\tilde{\sigma}_{e,n}$ and $\tilde{\sigma}_{g,n}$ for the nth molecule in the rotating frame at the laser frequency ω_ℓ:

$$\dot{a} = -(i\Delta_c + \kappa)a - ig\sum_{n=1}^{\mathcal{N}} \sigma_n + \sqrt{2\kappa_1}A_{1,\rm in} + \sqrt{2\kappa_2}a_{2,\rm in}, \tag{26a}$$

$$\dot{\tilde{\sigma}}_{e,n} \approx -(i\Delta_\ell + \gamma)\tilde{\sigma}_{e,n} + iga\mathcal{S}_{e,n}^\dagger \mathcal{D}_{e,n}^\dagger e^{i(v_e - v_g)b_{e,n}^\dagger b_{e,n} t} + \sqrt{2\gamma}\sigma_{{\rm in},n}\mathcal{S}_{e,n}^\dagger \mathcal{D}_{e,n}^\dagger e^{i(v_e - v_g)b_{e,n}^\dagger b_{e,n} t}, \tag{26b}$$

$$\dot{\tilde{\sigma}}_{g,n} \approx -(i\Delta_\ell + \gamma)\tilde{\sigma}_{g,n} - iga e^{i(v_e - v_g)b_{g,n}^\dagger b_{g,n} t}\mathcal{S}_{g,n}^\dagger \mathcal{D}_{g,n}^\dagger + \sqrt{2\gamma}e^{i(v_e - v_g)b_{g,n}^\dagger b_{g,n} t}\mathcal{S}_{g,n}^\dagger \mathcal{D}_{g,n}^\dagger \sigma_{{\rm in},n}. \tag{26c}$$

Here, the total dissipation for the cavity field $\kappa = \kappa_1 + \kappa_2$ encompasses the losses via both mirrors. The operator $A_{1,\rm in} = \eta_c/\sqrt{2\kappa_1} + a_{1,\rm in}$ describes the input classical field coming through the left mirror $\eta_c/\sqrt{2\kappa_1}$ and the zero-average input noise with the only nonvanishing two-time correlations $\langle a_{1,\rm in}(t)a_{1,\rm in}^\dagger(t')\rangle = \delta(t - t')$. Additionally, zero-average input noise comes through the right side mirror with similar correlations $\langle a_{2,\rm in}(t)a_{2,\rm in}^\dagger(t')\rangle = \delta(t - t')$ and uncorrelated with the $a_{1,\rm in}(t)$.

The Markovian limit is achieved under the large relaxation rate condition for the vibrational mode, i.e., $\Gamma \gg \kappa$ and $\Gamma \gg \gamma$. In this case, the approach to treat the vibrations as a local phonon bath is still applicable. By formally integrating

the equations for the polaron operator, tracing over the cavity mode as well as electronic degrees of freedom and taking the Laplace transformation, we have

$$\overline{\langle\sigma_n\rangle} = ig(\overline{\mathcal{G}}_{\rm em} + \overline{\mathcal{G}}_{\rm ab})\overline{\langle\mathcal{P}_{e,n}a\rangle} - ig\overline{\mathcal{G}}_{\rm ab}\overline{\langle a\rangle}. \tag{27}$$

The coupling between the cavity mode a and the projection operator $\mathcal{P}_{e,n}$ leads to nonlinear effects. However, we restrict our analysis to the weak excitation regime, i.e., the cavity photon number is much smaller than unity and the population of the excited electronic state $|e\rangle$ is negligible (under the condition that $\eta_c \ll \kappa$). In other words, this approximation allows for the construction of a linear-response theory formalism where the transmitted light gives information on the position and linewidths of the hybrid light-matter eigenstates of the system. In the case of identical conditions, the expectation value of the electronic coherence operator σ_n for the nth molecule will be equivalent to that of the other molecules, i.e., $\langle\sigma\rangle = \langle\sigma_n\rangle = \langle\sigma_m\rangle$ $(m \neq n)$. Then, the equations of motion are written in the vector form (in the Laplace transform domain) as $\overline{\mathbf{M}}\overline{\mathbf{v}} + \overline{\mathbf{v}}_c = 0$, with the drift matrix

$$\overline{\mathbf{M}} = \begin{pmatrix} -(i\Delta_c + \kappa) - s & -i\mathcal{N}g \\ -ig & -1/\overline{\mathcal{G}}_{\rm ab} \end{pmatrix}, \tag{28}$$

and the definitions $\mathbf{v} = (\langle a\rangle, \langle\sigma\rangle)^T$ and $\mathbf{v}_c = (\eta_c, 0)^T$. The diagonalization of the drift matrix (under resonance condition $\Delta_c = 0$) yields the frequencies $\omega_\pm$ and linewidths $\gamma_\pm$ [35,39] of the two polaritons as

$$\omega_\pm = \frac{-\Delta_{\rm eff}}{2} \pm \frac{1}{2}\mathcal{I}\sqrt{(\Gamma_{\rm eff} - \kappa + i\Delta_{\rm eff})^2 - \mathcal{N}g^2}, \tag{29a}$$

$$\gamma_\pm = \frac{\Gamma_{\rm eff} + \kappa}{2} \pm \frac{1}{2}\mathcal{R}\sqrt{(\Gamma_{\rm eff} - \kappa + i\Delta_{\rm eff})^2 - \mathcal{N}g^2}, \tag{29b}$$

with $\Gamma_{\rm eff} = \mathcal{R}\lim_{s\to 0} 1/\overline{\mathcal{G}}_{\rm ab}$ and $\Delta_{\rm eff} = \mathcal{I}\lim_{s\to 0} 1/\overline{\mathcal{G}}_{\rm ab}$ denoting the effective decay rate and additional frequency shift. These particularities of the polaritons can be explored in a very simple way by performing a scan of the laser frequency around the cavity resonance and noticing the position of the peaks corresponding to the hybrid light-matter states. This can be done at the analytical level in the weak excitation regime and compared to full exact numerics. We define the complex cavity transmission amplitude as the ratio of the normalized continuous outgoing field versus incoming field amplitudes,

$$\mathcal{T} = \frac{\sqrt{2\kappa_2}\langle a\rangle_{\rm SS}}{\eta_c/\sqrt{2\kappa_1}}, \tag{30}$$

and illustrate its behavior with respect to the scanning laser frequency in Fig. 5. The quantity $\langle a\rangle_{\rm SS}$ is the average value of the cavity mode amplitude in steady state in the linear-response regime:

$$\langle a\rangle_{\rm SS} = \frac{\eta_c}{\mathcal{N}g^2\chi_{\rm ab} + \kappa + i(\omega_c - \omega_\ell)}, \tag{31}$$

with $\chi_{\rm ab} = \lim_{s\to 0} 1/\overline{\mathcal{G}}_{\rm ab}$.

We illustrate numerical and analytical results in Fig. 5 where the profile of the cavity transmission at $\omega_c = \omega_{00}$ is plotted. The presence of the linear electron-vibron coupling scaling with λ_1 induces an interaction between upper and lower polaritons already presented at the theoretical level in a few treatments [1,7,8]. Instead, at the level of a single molecule, the quadratic interaction will suppress the polariton cross talk, as illustrated in Fig. 5(a). In essence, the squeezing term is responsible with a shift in the molecular resonance which then in turn brings the cavity off resonance with the electronic transition except the zero-phonon transition process. Increasing the number of molecules while assuming very weak driving conditions presents a different situation. This is shown in Fig. 5(b) as an effective reduction of the upper polariton with increasing particle number.

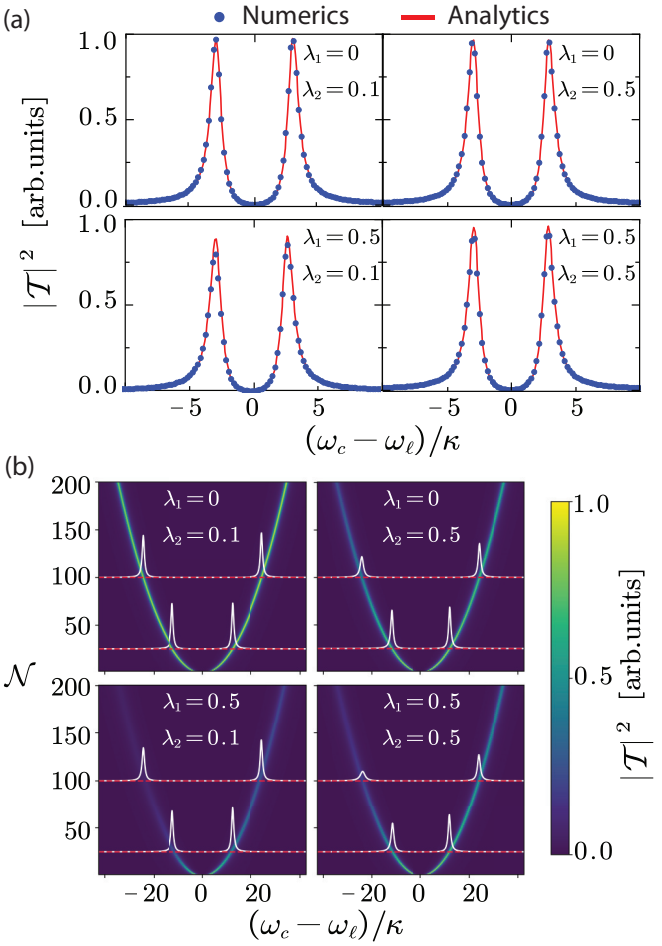

FIG. 5. Cavity transmission ($|\mathcal{T}|^2$) of the molecule with various linear and quadratic electron-vibron couplings λ_1 and λ_2 for a strong coupling to a single cavity mode. (a) Cavity transmission with a single molecule. (b) Cavity transmission as a function of the number of molecules in the cavity. The white lines represent the profile at $\mathcal{N} = 25$ and 100, respectively. Parameters: $\omega_c = \omega_{00}$, $g = 3\kappa$, $\nu_g = 10\kappa$, $\gamma = 0.01\kappa$, $\Gamma = 20\kappa$, $2\kappa_1 = 2\kappa_2 = \kappa$; the driving is assumed very weak $\eta_c/\kappa = 0.001$.

V. DISCUSSION AND CONCLUSIONS

In summary, we have applied the toolbox of open system dynamics and in particular the QLEs formalism to analytically describe spectroscopic properties of solid-state embedded molecules in free space or in optical cavity settings. In particular, we generalized our previous approach introduced in Ref. [7] to a scenario where the potential landscapes of a

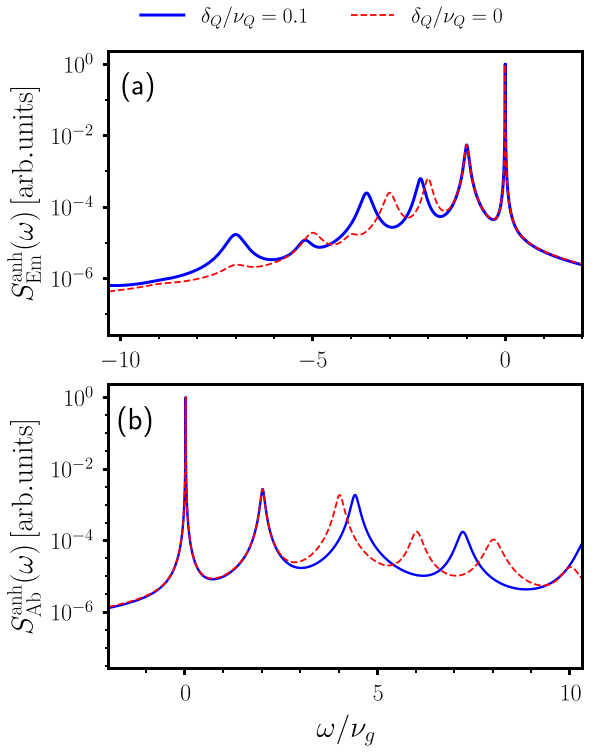

FIG. 6. Power spectra for (a) emission and (b) absorption processes with $\delta_Q/\nu_Q = 0.1$ (blue-solid) and $\delta_Q/\nu_Q = 0$ (red-dashed). The other parameters are the same as in Fig. 3.

molecule have unequal curvatures in the ground and excited electronic state. This has seen the introduction of a generalized polaron operator where the electronic degree of freedom is dressed by vibrations via a displacement operation followed by an additional squeezing operation. The first effect is seen in the emergent asymmetry between absorption and emission profiles for molecular spectroscopy. A second effect that emerges from our analytical calculations is the context of cavity quantum electrodynamics where the additional squeezing operation leads to a detuning between the bare molecular resonance and the cavity resonance. Our calculations can be relevant in the direction of optomechanics or optovibronics, owing to the strong electron-vibron couplings, albeit under very lossy conditions. Let us remark that the harmonic oscillator approximation for the potential landscapes proves rather robust owing to the high frequency of vibrational modes and their large relaxation rate. This can be easily observed by incorporating an anharmonic term in the Hamiltonian

$$\mathcal{H}^{Q}_{\rm anh} = \delta_Q b^\dagger_Q b^\dagger_Q b_Q b_Q, \tag{32}$$

both for ground and excited states $Q \in \{e, g\}$, an approach widely used in the literature [38,40,41]. The perturbation by $\mathcal{H}^{Q}_{\rm anh}$ affects the intrinsic frequencies of molecular vibrational energy levels and causes a shift in the central frequencies of the Lorentzian profiles $\gamma_m^{\uparrow/\downarrow}$ as shown in Fig. 6. Instead, the linewidth of the Lorentzian profile remains almost unchanged, indicating minimal additional dephasing effects on the electronic transition (see Appendix G for details). We remark that the primary determinant of the molecular vibration relaxation rates is the influence of the phonon reservoir in a solid-state environment, as discussed in Ref. [8]. However, owing to the high vibrational frequencies, experimental observations under cryogenic conditions confirm that the fluorescence is lifetime limited [42,43].

ACKNOWLEDGMENTS

We acknowledge financial support from the Max Planck Society and from Deutsche Forschungsgemeinschaft Grant No. 9429529648 under Project No. TRR 306 QuCoLiMa ("Quantum Cooperativity of Light and Matter"). M.A. was supported by Khalifa University of Science and Technology Grant No. FSU-2023-014.

APPENDIX A: THE MODIFIED HOLSTEIN HAMILTONIAN

Let us illustrate how the modified Holstein Hamiltonian arises, how it can be diagonalized, and how the quantum Langevin equations for the squeezed and displaced polaron operators can be derived.

1. First-principles derivation of the nonlinear Hamiltonian

We consider a single molecule with ground $|g\rangle$ (frequency ω_g) and excited $|e\rangle$ (frequency ω_e) electronic levels coupled to the ground phonons (ν_g) and the excited phonons (ν_e) of a single vibrational mode with mass μ respectively. Assume that the ground and excited electronic states have different parabolic shape around the minima. Then the total Hamiltonian of the electron-phonon system reads as ($\hbar = 1$)

$$\begin{aligned}\mathcal{H} &= \left[\omega_e + \frac{\hat{P}^2}{2\mu} + \frac{1}{2}\mu\nu_e^2(\hat{R} - R_{eg})^2\right]\sigma^\dagger\sigma + \left(\omega_g + \frac{\hat{P}^2}{2\mu} + \frac{1}{2}\mu\nu_g^2\hat{R}^2\right)\sigma\sigma^\dagger \\ &= \omega_g\sigma\sigma^\dagger + \left(\omega_e + \mu\nu_e^2R_{eg}^2/2\right)\sigma^\dagger\sigma + \frac{\hat{P}^2}{2\mu} + \frac{1}{2}\mu\nu_g^2\hat{R}^2 + \frac{1}{2}\mu\nu_e^2R_{eg}\hat{R}\sigma^\dagger\sigma + \frac{1}{2}\mu\left(\nu_e^2 - \nu_g^2\right)\hat{R}^2\sigma^\dagger\sigma,\end{aligned} \tag{A1}$$

where $\sigma = |g\rangle\langle e|$ is the Pauli lowering operator. By rewriting position ($\hat{R}$) and momentum ($\hat{P}$) in terms of creation $b^\dagger = (\hat{R}/R_{\rm ZPM} - iR_{\rm ZPM}\hat{P})/\sqrt{2}$ and annihilation $b = (\hat{R}/R_{\rm ZPM} + iR_{\rm ZPM}\hat{P})/\sqrt{2}$ operators that fulfill $[b, b^\dagger] = 1$, the Hamiltonian in Eq. (A1) can be written as

$$\begin{aligned}\mathcal{H} = \omega_0\sigma^\dagger\sigma + \nu_g b^\dagger b + \lambda_1\nu_g(b + b^\dagger)\sigma^\dagger\sigma \\ + \lambda_2\nu_g(b + b^\dagger)^2\sigma^\dagger\sigma,\end{aligned} \tag{A2}$$

where $\omega_0 = \omega_e - \omega_g + \mu\nu_e^2 R_{\rm eg}^2/2 = \omega_e - \omega_g + \lambda_1^2\nu_g^3/\nu_e^2$ is the modified frequency of the electronic excited state. $\lambda_1 = \mu\nu_e^2 R_{eg}R_{\rm ZPM}/\nu_g$ and $\lambda_2 = (\nu_e^2 - \nu_g^2)/4\nu_g^2$ are the linear and quadratic coupling constants.

2. Quadratic Holstein Hamiltonian diagonalization

In the presence of both linear and quadratic couplings, the diagonalization of the Hamiltonian in Eq. (3) can be achieved by performing a sequence of unitary transformations. This transformation could be accomplished by first removing all the linear terms via the polaron transformation $\mathcal{U}_d = [\mathcal{D}(r_d)]^{\sigma^\dagger\sigma} = \sigma\sigma^\dagger + \mathcal{D}(r_d)\sigma^\dagger\sigma$, where the displacement operator is defined as $\mathcal{D}(r_d) = \exp[r_d(b^\dagger - b)]$. The polaron transformation has the effect that $b \to \mathcal{U}_d^\dagger b\mathcal{U}_d = b + r_d\sigma^\dagger\sigma$. Specifically, when

$$r_d = -\frac{\lambda_1}{1+4\lambda_2} = -\lambda_1\frac{\nu_g^2}{\nu_e^2}, \tag{A3}$$

the resulting Hamiltonian $\mathcal{H}_1 = \mathcal{U}_d^\dagger\mathcal{H}\mathcal{U}_d$ can be written as

$$\mathcal{H}_1 = \left[\omega_0 + r_d^2\nu_g(1+4\lambda_2) + 2\lambda_1 r_d\right]\sigma^\dagger\sigma + \nu_g b^\dagger b + \lambda_2\nu_g(b+b^\dagger)^2\sigma^\dagger\sigma. \tag{A4}$$

We now diagonalize this Hamiltonian via squeezing transformation $\mathcal{U}_s = [\mathcal{S}(r_s)]^{\sigma^\dagger\sigma} = \sigma\sigma^\dagger + \mathcal{S}(r_s)\sigma^\dagger\sigma$, where $\mathcal{S}(r_s) = \exp[r_s(b^2 - b^{\dagger 2})/2]$ is a single mode squeezing operator, so as to remove the quadratic terms. Under this transformation $b \to \mathcal{U}_s^\dagger b\mathcal{U}_s = b\sigma\sigma^\dagger + [b\cosh(r_s) + b^\dagger\sinh(r_s)]\sigma^\dagger\sigma$, the resulting Hamiltonian $\mathcal{H}_2 = \mathcal{U}_s^\dagger\mathcal{H}_1\mathcal{U}_s$ can be written as

$$\mathcal{H}_2 = \nu_g b^\dagger b\sigma\sigma^\dagger + \nu_e b^\dagger b\sigma^\dagger\sigma + \omega_{00}\sigma^\dagger\sigma \tag{A5}$$

under the condition of

$$e^{4r_s} = 1 + 4\lambda_2 = \frac{\nu_e^2}{\nu_g^2}. \tag{A6}$$

Here $\omega_{00} = \omega_0 + r_d\lambda_1\nu_g + (\nu_e - \nu_g)/2$ is the zero-phonon line. This transformation could be also accomplished in a reverse order, by first removing quadratic terms under applying $\mathcal{U}_s' = [\mathcal{S}(r_s)]^{\sigma^\dagger\sigma}$ and then removing the all linear terms via polaron transformation $\mathcal{U}_d' = [\mathcal{D}(r_d e^{r_s})]^{\sigma^\dagger\sigma}$. The results are, of course, identical.

APPENDIX B: DERIVATION OF THE EFFECTIVE QUANTUM LANGEVIN EQUATIONS FOR THE ELECTRONIC TRANSITION

1. Effective quantum Langevin equation for the vibrational mode

Let us consider one special case where the relaxation rate for the vibrations is much larger than the rate of change for the population on the electric excited state. Then the dynamical behaviors for vibrations with molecules populating on the state $|e\rangle$ tend to be different from those with molecules occupying in the state $|g\rangle$. This fact motivates the partitioning of the total Hilbert space into the orthogonal subspaces via the following two projection operators:

$$\mathcal{P}_e = \sigma^\dagger\sigma \quad \text{and} \quad \mathcal{P}_g = \sigma\sigma^\dagger. \tag{B1}$$

The bosonic annihilation operator can thus be partitioned into $b = b\sigma^\dagger\sigma + b\sigma\sigma^\dagger$, which gives two dynamical equations corresponding to the operator $b_1 = b\sigma^\dagger\sigma$ and $b_2 = b\sigma\sigma^\dagger$ as

$$\dot{b}_1 = b\frac{d}{dt}(\sigma^\dagger\sigma) - [i(1+2\lambda_2)\nu_g + \Gamma]b_1 - i\lambda_1\nu_g\sigma^\dagger\sigma - i2\lambda_2\nu_g b_1^\dagger + \Gamma r_d\mathcal{P}_e + \sqrt{2\Gamma}\mathcal{B}_1^{\rm in}\mathcal{P}_e, \tag{B2a}$$

$$\dot{b}_2 = -b\frac{d}{dt}(\sigma^\dagger\sigma) - (i\nu + \Gamma)b_2 + \sqrt{2\Gamma}\mathcal{B}_2^{\rm in}\mathcal{P}_g, \tag{B2b}$$

where $\mathcal{B}_1^{\rm in}$ and $\mathcal{B}_2^{\rm in}$ are the noise operators.

Assuming a large relaxation rate for the vibrational mode, the evolution of $\sigma^\dagger\sigma$ can be approximately negligible, while the vibrational mode rapidly relaxes to the steady situation. Then we can get the effective dynamical equations of b_1 and b_2:

$$\dot{b}_1 \approx 1 - [i(1+2\lambda_2)\nu_g + \Gamma]b_1 - i\lambda_1\nu_g\mathcal{P}_e - i2\lambda_2\nu_g b_1^\dagger + \Gamma r_d\mathcal{P}_e + \sqrt{2\Gamma}\mathcal{B}_1^{\rm in}\mathcal{P}_e, \tag{B3a}$$

$$\dot{b_2}1 \approx 1 - (i\nu + \Gamma)b_2 + \sqrt{2\Gamma}\mathcal{B}_2^{\rm in}\mathcal{P}_g. \tag{B3b}$$

By introducing $b_e = \mathcal{U}b_1\mathcal{U}^\dagger = \cosh r_s b_1 + \sinh r_s b_1^\dagger - r_d\exp(r_s)\mathcal{P}_e$, one can get the effective Langevin equation for b_e:

$$\frac{d}{dt}b_e = -(i\nu_e + \Gamma)b_e + \sqrt{2\Gamma}\mathcal{B}_{\rm e}^{\rm in}\mathcal{P}_e. \tag{B4}$$

Under the condition $\Gamma \gg \gamma$, and $\Gamma \gg \eta_\ell$, one can assume the correlation between noise operators $\mathcal{B}_e^{\rm in}$ and $\mathcal{B}_g^{\rm in}$ is negligible as

$$\left\langle\mathcal{B}_e^{\rm in\dagger}(t)\mathcal{B}_g^{\rm in}(\tau)\right\rangle \approx 0 \quad \text{and} \quad \left\langle\mathcal{B}_g^{\rm in\dagger}(t)\mathcal{B}_e^{\rm in}(\tau)\right\rangle \approx 0, \tag{B5}$$

and the nonvanishing correlation functions obey the fluctuation-dissipation relation:

$$\left\langle\mathcal{B}_e^{\rm in\dagger}(t)\mathcal{B}_e^{\rm in}(\tau)\right\rangle = \delta(t-\tau) \quad \text{and} \quad \left\langle\mathcal{B}_g^{\rm in\dagger}(t)\mathcal{B}_g^{\rm in}(\tau)\right\rangle = \delta(t-\tau). \tag{B6}$$

2. Effective quantum Langevin equation for the electronic transition

Let us pay attention to the electronic transition by introducing the "dressed" dipole operator, i.e., polaron operator, $\tilde{\sigma}_e' = \sigma\mathcal{S}_1^\dagger\mathcal{D}_1^\dagger$. The Langevin equation $\dot{\tilde{\sigma}}_e' = \dot{\sigma}\mathcal{S}_1^\dagger\mathcal{D}_1^\dagger + \sigma\,\partial_t(\mathcal{S}_1^\dagger\mathcal{D}_1^\dagger)$

in a rotating frame at driving frequency ω_ℓ can be expressed as

$$\dot{\tilde{\sigma}}'_e \approx -[i(\omega_{00}-\omega_\ell)+\gamma]\tilde{\sigma}'_e - \eta_\ell \mathcal{S}_1^\dagger \mathcal{D}_1^\dagger \sigma^\dagger \sigma + \sqrt{2\gamma}\sigma_{\rm in}\mathcal{S}_1^\dagger\mathcal{D}_1^\dagger - i\left(1-\frac{\nu_g}{\nu_e}\right)\tilde{\sigma}'_e[\nu_g b_1^\dagger b_1 + \lambda_1\nu_g(b_1+b_1^\dagger)+\lambda_2\nu_g(b_1+b_1^\dagger)^2], \quad \text{(B7)}$$

with $\mathcal{S}_1 = \exp[r_s(b_1^2 - b_1^{\dagger 2})/2]\mathcal{P}_e$ and $\mathcal{D}_1 = \exp[r_d(b_1^\dagger - b_1)]\mathcal{P}_e$.

Considering that the quadratic terms in the second line of the equation above, i.e., $\nu_g b_1^\dagger b_1 + \lambda_1\nu_g(b_1+b_1) + \lambda_2\nu_g(b_1+b_1^\dagger)^2$, can be reformed as $\nu_e b_e^\dagger b_e$, where the definition of b_e is introduced in Eq. (B4), we can thus reform the equation above into

$$\dot{\tilde{\tilde{\sigma}}}_e \approx -[i(\omega_{00}-\omega_\ell)+\gamma]\tilde{\tilde{\sigma}}_e - i(\nu_e-\nu_g)\tilde{\tilde{\sigma}}_e b_e^\dagger b_e - \eta_\ell \mathcal{S}_e^\dagger\mathcal{D}_e^\dagger\sigma^\dagger\sigma + \sqrt{2\gamma}\sigma_{\rm in}\mathcal{S}_e^\dagger\mathcal{D}_e^\dagger, \quad \text{(B8)}$$

with $\tilde{\tilde{\sigma}}_e = \sigma\mathcal{S}_e^\dagger\mathcal{D}_e^\dagger$, $\mathcal{S}_e = \exp[(r_s(b^2-b^{\dagger 2})/2)\sigma^\dagger\sigma]\mathcal{P}_e$, and $\mathcal{D}_e = \exp[r_d(b^\dagger - b)\sigma^\dagger\sigma]\mathcal{P}_e$.

Taking into account the dynamical equation for $\exp[i(\nu_e-\nu_g)b_e^\dagger b_e t]$ given by

$$\begin{aligned}\frac{d}{dt}e^{i(\nu_e-\nu_g)b_e^\dagger b_e t} &= i(\nu_e-\nu_g)\int_0^1 e^{i\alpha(\nu_e-\nu_g)b_e^\dagger b_e t}\frac{d}{dt}(b_e^\dagger b_e t)e^{i(1-\alpha)i(\nu_e-\nu_g)b_e^\dagger b_e t}d\alpha \\ &= i(\nu_e-\nu_g)b_e^\dagger b_e e^{i(\nu_e-\nu_g)b_e^\dagger b_e t} + i(\nu_e-\nu_g)t\left[-2\Gamma b_e^\dagger b_e + \sqrt{2\Gamma}\frac{e^{i(\nu_e-\nu_g)t}-1}{i(\nu_e-\nu_g)t}b_e^\dagger \mathcal{B}_{\rm e}^{\rm in} + \text{H.c.}\right], \end{aligned} \quad \text{(B9)}$$

one can recast Eq. (B8) into

$$\begin{aligned}\dot{\tilde{\sigma}}_e \approx &-[i(\omega_{00}-\omega_\ell)+\gamma]\tilde{\sigma}_e - \eta_\ell\mathcal{S}_e^\dagger\mathcal{D}_e^\dagger e^{i(\nu_e-\nu_g)b_e^\dagger b_e t}\sigma^\dagger\sigma \\ &+\sqrt{2\gamma}\sigma_{\rm in}\mathcal{S}_e^\dagger\mathcal{D}_e^\dagger e^{i(\nu_e-\nu_g)b_e^\dagger b_e t}, \end{aligned} \quad \text{(B10)}$$

with $\tilde{\sigma}_e = \tilde{\tilde{\sigma}}_e\exp[(i\nu_e - i\nu_g)b_e^\dagger b_e t]$. Here, we have dropped the second term on the right side of Eq. (B9) to obtain the equation above and to receive a sufficient approximation.

Notably, Eq. (B8) only concludes the contribution of the vibrations projecting to the manifold of $\mathcal{P}_e$. To get the dynamics of the system in the whole Hilbert space, one also needs to get the dynamics of the general polaron operator $\tilde{\tilde{\sigma}}_g = \mathcal{S}_g^\dagger\mathcal{D}_g^\dagger\sigma$ for the vibrational mode projecting to the manifold of $\mathcal{P}_g$ with $\mathcal{S}_g = \exp[r_s(b_g - b_g^{\dagger 2})/2]\mathcal{P}_g$, and $\mathcal{D}_g = [r_d(b_g - b_g^\dagger)]\mathcal{P}_g$:

$$\begin{aligned}\dot{\tilde{\tilde{\sigma}}}_g \approx &-[i(\omega_{00}-\omega_\ell)+\gamma]\tilde{\tilde{\sigma}}_g - i(\nu_e-\nu_g)b_g^\dagger b_g\tilde{\tilde{\sigma}}_g \\ &+\eta_\ell\mathcal{S}_g^\dagger\mathcal{D}_g^\dagger\sigma\sigma^\dagger + \sqrt{2\gamma}\sigma_{\rm in}\mathcal{S}_g^\dagger\mathcal{D}_g^\dagger\sigma\sigma^\dagger. \end{aligned} \quad \text{(B11)}$$

Repeating the process to derive the dynamical equation of $\tilde{\sigma}_e$, one can recast the above equation into

$$\begin{aligned}\dot{\tilde{\sigma}}_g \approx &-[i(\omega_{00}-\omega_\ell)+\gamma]\tilde{\sigma}_g + e^{i(\nu_e-\nu_g)b_g^\dagger b_g t}\eta_\ell\mathcal{S}_g^\dagger\mathcal{D}_g^\dagger\sigma\sigma^\dagger \\ &+\sqrt{2\gamma}\sigma_{\rm in}e^{i(\nu_e-\nu_g)b_g^\dagger b_g t}\mathcal{S}_g^\dagger\mathcal{D}_g^\dagger\sigma\sigma^\dagger, \end{aligned} \quad \text{(B12)}$$

with $\tilde{\sigma}_g = \exp[(i\nu_e - i\nu_g)b_g^\dagger b_g t]\tilde{\tilde{\sigma}}_g$.

Meanwhile, one can also get the dynamical equation for the population of the excited state, given by

$$\frac{d}{dt}\sigma^\dagger\sigma = -2\gamma\sigma^\dagger\sigma + \eta_\ell(\sigma+\sigma^\dagger) + \sqrt{2\gamma}(\sigma^\dagger\sigma_{\rm in} + \sigma\sigma_{\rm in}^\dagger). \quad \text{(B13)}$$

APPENDIX C: VIBRATIONAL DYNAMICS

As discussed in the previous section, the electronic transition is dressed by vibrations. For the further calculation of the electronic transition, we here analyze the properties of vibrations and derive the expression for the two time-correlation terms for the product of squeezing and displacement operators $\mathcal{S}_g^\dagger\mathcal{D}_g^\dagger$ and $\mathcal{S}_e^\dagger\mathcal{D}_e^\dagger$.

1. Nonlinear vibrational dynamics

In the previous section, we have derived the effective Langevin equation (B4) describing the dynamics of the vibrational mode projected onto the manifold of $\mathcal{P}_e$. One can easily obtain the exact solution of such an equation, which is given by

$$b_e = \sqrt{2\Gamma}\int_{-\infty}^{t} d\tau\, e^{-(i\nu_e+\Gamma)(t-\tau)}\mathcal{B}_e^{\rm in}(\tau)\mathcal{P}_e(\tau). \quad \text{(C1)}$$

Due to the correlation time for vibrations being much shorter than for the electronic transitions, the quantity for $\sigma^\dagger\sigma(\tau)$ varies little around $\sigma^\dagger\sigma(t)$. We can thus proceed via a Markov approximation by taking it out of the integral, which yields

$$b_e = \sqrt{2\Gamma}\mathcal{P}_e(t)\int_{-\infty}^{t} d\tau\, e^{-(i\nu_e+\Gamma)(t-\tau)}\mathcal{B}_e^{\rm in}(\tau). \quad \text{(C2)}$$

With this, we can derive the two-time correlation for $t > \tau$:

$$\langle b_e(t)b_e^\dagger(\tau)\rangle_{\rm vib} = e^{-(i\nu_e+\Gamma)(t-\tau)}\mathcal{P}_e(t), \quad \text{(C3a)}$$

$$\langle b_e(\tau)b_e^\dagger(t)\rangle_{\rm vib} = e^{-(-i\nu_e+\Gamma)(t-\tau)}\mathcal{P}_e(t), \quad \text{(C3b)}$$

where $\langle\cdot\rangle_{\rm vib}$ denotes taking the average over the degrees of freedom of the vibrational mode.

Similar to the case for calculating b_e, we can obtain the two-time correlation term for the vibrational operator b_g projected onto the manifold of $\mathcal{P}_g$ as

$$\langle b_g(t)b_g^\dagger(\tau)\rangle_{\rm vib} = e^{-(i\nu_g+\Gamma)(t-\tau)}\sigma\sigma^\dagger(t), \quad \text{(C4a)}$$

$$\langle b_g(\tau)b_g^\dagger(t)\rangle_{\rm vib} = e^{(i\nu_g-\Gamma)(t-\tau)}\sigma\sigma^\dagger(t). \quad \text{(C4b)}$$

Thus, the two-time correlation function for the vibrational mode in the whole Hilbert space reads

$$\begin{aligned}\langle b(t+\tau)b^\dagger(t)\rangle \approx &\langle b_g(\tau)b_g^\dagger(0)\rangle + \langle b_e(\tau)b_e^\dagger(0)\rangle \\ \approx &e^{-(i\nu_g+\Gamma)(\tau)}\langle\sigma\sigma^\dagger(t)\rangle + e^{-(i\nu_e+\Gamma)(\tau)} \\ &\times\ \langle\sigma^\dagger\sigma(t)\rangle. \end{aligned} \quad \text{(C5)}$$

Here, the correlations between different manifolds have been properly dropped because of the much smaller value for such

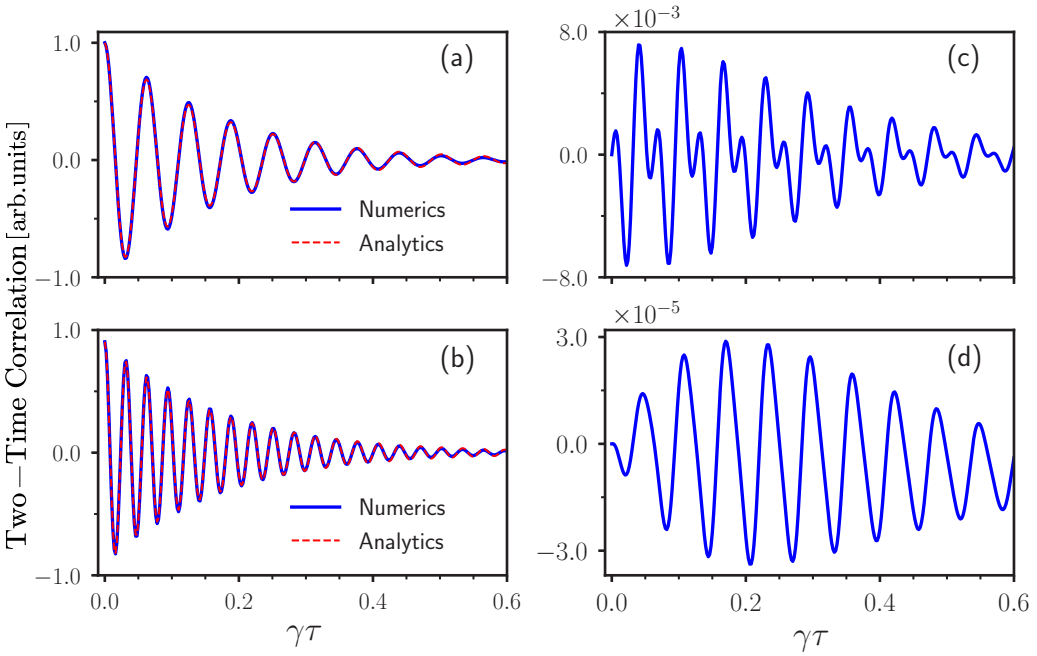

FIG. 7. Normalized two-time correlation function in steady state for (a) $\langle b_g(\tau)b_g^\dagger(0)\rangle$, (b) $\langle b_e(\tau)b_e^\dagger(0)\rangle$, (c) $\langle b_e(\tau)b_g^\dagger(0)\rangle$, and (d) $\langle b_g(\tau)b_e^\dagger(0)\rangle$. The blue-solid lines in (a)–(d) are generated with the toolbox QUTIP [44] under the following parameters $\nu_g = 1$, $\nu_e/\nu_g = 2$, $\Gamma/\nu_g = 0.1$, $\gamma/\nu_g = 0.01$, and $\eta_\ell/\gamma = 2$. The red-dashed lines in (a) and (b) are calculated via the first and the second term in the right side of Eq. (C5), respectively.

terms $\langle b_e(\tau)b_g^\dagger(0)\rangle$ and $\langle b_g(\tau)b_e^\dagger(0)\rangle$ comparing with that in the same manifold, as illustrated in Fig. 7.

2. Two-time correlation function for the displacement-squeezing operator

Using that the squeezing operator can be written in a disentangled form as

$$\mathcal{S} = \exp\left[-\tfrac{1}{2}\tanh r_s b^{\dagger 2}\right]\exp\left[-\ln\cosh r_s\left(b^\dagger b + \tfrac{1}{2}\right)\right] \times \exp\left[\tfrac{1}{2}\tanh r_s b^2\right], \tag{C6}$$

we can calculate the two-time correlation function for the displacement-squeezing operator under the vacuum state. For instance, the two-time correlation for the manifold of $\mathcal{P}_e$ is given by

$$\langle \mathcal{S}_e^\dagger(\tau)\mathcal{D}_e^\dagger(\tau)\mathcal{D}_e(t)\mathcal{S}_e(t)\rangle_{\rm vib} = \frac{e^{-r_d^2\alpha}}{\cosh(r_s)}\left\langle e^{-\beta b_e^2(\tau)}e^{\alpha r_d b_e(\tau)}e^{\alpha r_d b_e^\dagger(t)}e^{-\beta b_e^{\dagger 2}(t)}\right\rangle_{\rm vib}, \tag{C7}$$

with $\alpha = \tanh r_s + 1 = 2\nu_e/(\nu_e+\nu_g)$ and $\beta = (\tanh r_s)/2$.

Using the generating function of the Hermite polynomials given by

$$e^{2x\varphi-\varphi^2} = \sum_{n=0}^{\infty} H_n(x)\frac{\varphi^n}{n!}, \tag{C8}$$

we can expand the first and second exponential in the equation above in terms of Hermite polynomials with $x = \alpha r_d/(2\sqrt{\beta})$ and $\varphi = \sqrt{\beta}b_e$. Thus, we finally obtain the expression for the two-time correlation function under the Isserlis theorem:

$$\langle \mathcal{S}_e^\dagger(\tau)\mathcal{D}_e^\dagger(\tau)\mathcal{D}_e(t)\mathcal{S}_e(t)\rangle_{\rm vib} = \mathcal{F}_{\rm em}(-\nu_e, t-\tau)\mathcal{P}_e(t), \tag{C9}$$

where

$$\mathcal{F}_{\rm em}(\nu,t) = \sum_{m=0}^{\infty} S_m^{\rm em} e^{-m(i\nu+\Gamma)t}, \tag{C10a}$$

$$S_m^{\rm em} = \frac{e^{-r_d^2\alpha}}{\cosh(r_s)}\left[H_m\left(\frac{\alpha r_d}{2\sqrt{\beta}}\right)\right]^2\frac{\beta^m}{m!}. \tag{C10b}$$

Of course, we can obtain the result for the following equation in the same way:

$$\left\langle \mathcal{S}_e^\dagger(\tau)\mathcal{D}_e^\dagger(\tau)e^{i(\nu_e-\nu_g)b_e^\dagger b_e\tau}e^{-i(\nu_e-\nu_g)b_e^\dagger b_e t}\mathcal{D}_e(t)\mathcal{S}_e(t)\right\rangle_{\rm vib} = \mathcal{F}_{\rm em}(-\nu_g, t-\tau)\mathcal{P}_e(t). \tag{C11}$$

The two-time correlation in the manifold of $\mathcal{P}_g$ reads

$$\langle \mathcal{D}_g(t)\mathcal{S}_g(t)\mathcal{S}_g^\dagger(\tau)\mathcal{D}_g^\dagger(\tau)\rangle_{\rm vib} = \mathcal{F}_{\rm ab}(\nu_g, t-\tau)\mathcal{P}_g(t), \tag{C12}$$

and also

$$\langle \mathcal{D}_g(t)\mathcal{S}_g(t)e^{-i(\nu_e-\nu_g)b_g^\dagger b_g t}e^{i(\nu_e-\nu_g)b_g^\dagger b_g\tau}\mathcal{S}_g^\dagger(\tau)\mathcal{D}_g^\dagger(\tau)\rangle_{\rm vib} = \mathcal{F}_{\rm ab}(\nu_e, t-\tau)\mathcal{P}_g(t), \tag{C13}$$

where

$$\mathcal{F}_{\rm ab}(\nu,t) = \sum_{m=0}^{\infty} S_m^{\rm ab} e^{-m(i\nu+\Gamma)t}, \tag{C14a}$$

$$S_m^{\rm ab} = \frac{e^{\alpha r_d^2\exp(2r_s)}}{\cosh(r_s)}\left[H_m\left(-\frac{i\alpha r_d\exp(r_s)}{2\sqrt{\beta}}\right)\right]^2\frac{(-\beta)^m}{m!}, \tag{C14b}$$

with $\alpha = \tanh r_s - 1 = -2\nu_g/(\nu_e+\nu_g)$.

APPENDIX D: STABILITY ANALYSIS

It is straightforward to obtain the expression for the Pauli operator in the whole Hilbert space by formally integrating Eqs. (B10) and (B12):

$$\sigma(t) = \int_0^t d\tau\,[-\eta_\ell + \sqrt{2\Gamma}\sigma_{\rm in}(\tau)]e^{[-i(\omega_{00}-\omega_\ell)-\gamma](t-\tau)}\mathcal{S}_e^\dagger(\tau)\mathcal{D}_e^\dagger(\tau)e^{i(\nu_e-\nu_g)b_e^\dagger b_e\tau}e^{-i(\nu_e-\nu_g)b_e^\dagger b_e t}\mathcal{D}_e(t)\mathcal{S}_e(t)$$
$$+\int_0^t d\tau\,[\eta_\ell + \sqrt{2\Gamma}\sigma_{\rm in}(\tau)]e^{[-i(\omega_{00}-\omega_\ell)-\gamma](t-\tau)}\mathcal{D}_g(t)\mathcal{S}_g(t)e^{-i(\nu_e-\nu_g)b_g^\dagger b_g t}e^{i(\nu_e-\nu_g)b_g^\dagger b_g\tau}\mathcal{S}_g^\dagger(\tau)\mathcal{D}_g^\dagger(\tau), \tag{D1}$$

with the initial value $\sigma(0) = 0$.

Under the assumption that the correlation time for the vibrations is much shorter than that for the electronic transition, we can treat the vibrations as a Markovian phonon bath. By taking the average of the vibrational mode and substituting Eq. (C11) as well as Eq. (C13) into the equation above, we then obtain

$$\sigma(t) = \int_0^\infty d\tau\,[-\eta_\ell + \sqrt{2\Gamma}\sigma_{\rm in}(\tau)]\mathcal{G}_{\rm em}(-\nu_g, t-\tau)\mathcal{P}_e(\tau) + \int_0^\infty d\tau\,[\eta_\ell + \sqrt{2\Gamma}\sigma_{\rm in}(\tau)]\mathcal{G}_{\rm ab}(\nu_e, t-\tau)\mathcal{P}_g(\tau), \tag{D2}$$

with $\mathcal{G}_Q(\nu,\tau) = \exp[(i\omega_\ell - i\omega_{00} - \gamma)(t-\tau)]\mathcal{F}_Q(\nu, t-\tau)\Theta(t-\tau)$ and $Q \in \{\text{em}, \text{ab}\}$, where $\Theta(t)$ is the Heaviside step function.

Tracing over the electronic transition, we finally obtain the simplified formal solution for $\langle\sigma\rangle$ as

$$\langle\sigma(t)\rangle = -\eta_\ell\int_0^\infty d\tau\,\mathcal{G}_{\rm em}(-\nu_g, t-\tau)P_e(\tau)$$
$$+\eta_\ell\int_0^\infty d\tau\,\mathcal{G}_{\rm ab}(\nu_e, t-\tau)[1-P_e(\tau)], \tag{D3}$$

with the population of the electronic excited state $P_e = \langle\sigma^\dagger\sigma\rangle$.

We proceed with our calculation via the Laplace transformation [defined as $\overline{f}(s) = \int_0^\infty dt\, f(t)\exp(-st)$ for a time-dependent function $f(t)$ at $t \geqslant 0$]. Then Eq. (D3) can be written in the Laplace domain as

$$\overline{\langle\sigma\rangle} = \frac{\eta_\ell}{s}\overline{\mathcal{G}}_{\rm ab} - \eta_\ell\overline{P}_e(\overline{\mathcal{G}}_{\rm ab} + \overline{\mathcal{G}}_{\rm em}), \tag{D4}$$

where $\overline{\mathcal{G}}_{\rm em}$ and $\overline{\mathcal{G}}_{\rm ab}$ are the Laplace transform of $\mathcal{G}_{\rm ab}(\nu_e, t)$ and $\mathcal{G}_{\rm em}(-\nu_g, t)$, expressed as

$$\overline{\mathcal{G}}_{\rm ab} = \sum_{m=0}^\infty \frac{S_m^{\rm ab}}{s + m\Gamma + \gamma + i(\omega_{00} - \omega_\ell + m\nu_e)}, \tag{D5a}$$

$$\overline{\mathcal{G}}_{\rm em} = \sum_{m=0}^\infty \frac{S_m^{\rm em}}{s + \gamma + m\Gamma + i(\omega_{00} - \omega_\ell - m\nu_g)}. \tag{D5b}$$

Assuming that the molecule is prepared in the electronic ground state $|g\rangle$ followed by taking an average over the electronic transition on both sides of Eq. (B13), and applying the Laplace transformation, we finally obtain

$$s\overline{P}_e = -2\gamma\overline{P_e} + \eta_\ell(\overline{\langle\sigma\rangle} + \overline{\langle\sigma\rangle}^*). \tag{D6}$$

Plugging Eq. (D6) into Eq. (D3), we can get

$$\overline{\langle\sigma\rangle} = \frac{i2\eta_\ell^3\mathcal{I}[\overline{\mathcal{G}}_{\rm ab}\overline{\mathcal{G}}_{\rm em}^*] + \eta_\ell(s+2\gamma)\overline{\mathcal{G}}_{\rm ab}}{s\big(2\gamma + s + 2\eta_\ell^2\mathcal{R}[\overline{\mathcal{G}}_{\rm ab} + \overline{\mathcal{G}}_{\rm em}]\big)}, \tag{D7a}$$

$$\overline{P}_e = \frac{2\eta_\ell^2}{s\big(2\gamma + s + 2\eta_\ell^2\mathcal{R}[\overline{\mathcal{G}}_{\rm ab} + \overline{\mathcal{G}}_{\rm em}]\big)}\mathcal{R}[\overline{\mathcal{G}}_{\rm ab}], \tag{D7b}$$

where $\mathcal{I}[\cdot]$ and $\mathcal{R}[\cdot]$ denote taking the imaginary and real part, respectively. According to the final value theorem, we get the steady values

$$\langle\sigma\rangle_{\rm SS} = \lim_{s\to0} s\overline{\langle\sigma\rangle} = \frac{i\eta_\ell^3\mathcal{I}[\chi_{\rm ab}\chi_{\rm em}^*] + \eta_\ell\gamma\chi_{\rm ab}}{\gamma + \eta_\ell^2\mathcal{R}[\chi_{\rm ab} + \chi_{\rm em}]}, \tag{D8a}$$

$$P_e^{\rm SS} = \lim_{s\to0} s\overline{P}_e = \frac{\eta_\ell^2}{\gamma + \eta_\ell^2\mathcal{R}[\chi_{\rm ab} + \chi_{\rm em}]}\mathcal{R}[\chi_{\rm ab}], \tag{D8b}$$

with $\chi_Q = \lim_{s\to0}\overline{\mathcal{G}}_Q$. In the limit of weak driving $\eta_\ell \ll \gamma$, the equation above can be simplified to

$$\langle\sigma\rangle_{\rm SS} \to \eta_\ell\chi_{\rm ab} = \sum_{m=0}^\infty \frac{S_m^{\rm ab}}{m\Gamma + \gamma + i(\omega_{00} - \omega_\ell + m\nu_e)}, \tag{D9a}$$

$$P_e^{\rm SS} \to \frac{\eta_\ell^2}{\gamma}\mathcal{R}[\chi_{\rm ab}] = \frac{\eta_\ell^2}{\gamma}\sum_{m=0}^\infty \frac{S_m^{\rm ab}(m\Gamma+\gamma)}{(m\Gamma+\gamma)^2 + (\omega_{00} - \omega_\ell + m\nu_e)^2}. \tag{D9b}$$

APPENDIX E: RATE EQUATION

For large vibrational relaxation rates $\Gamma \gg \eta_\ell$, the electronic transition is usually going from the lowest vibrational state in both electronic states $|g\rangle$ and $|e\rangle$. Thus, the motion of the population p_m^e on the state $|e; m_e\rangle$ as well as the population p_m^g on the state $|g; m_g\rangle$ are given phenomenology by

$$\begin{aligned}
\partial_t p_m^e &= 2\gamma_m^\uparrow p_0^g + \Gamma p_{m+1}^e - \Gamma p_m^e,\\
\partial_t p_{m-1}^e &= 2\gamma_{m-1}^\uparrow p_0^g + \Gamma p_m^e - \Gamma p_{m-1}^e,\\
&\vdots\\
\partial_t p_0^e &= 2\gamma_0^\uparrow p_0^g + \Gamma p_0^e - 2\gamma p_0^e - 2\sum_{m=0}^\infty \gamma_m^\downarrow p_0^e,\\
\partial_t p_m^g &= 2\gamma_m^\downarrow p_0^e + 2\gamma_m p_0^e + \Gamma p_{m+1}^g - \Gamma p_m^g,\\
\partial_t p_{m-1}^e &= 2\gamma_{m-1}^\downarrow p_0^e + 2\gamma_{m-1} p_0^e + \Gamma p_m^g - \Gamma p_{m-1}^g,\\
&\vdots\\
\partial_t p_0^g &= 2\gamma_0^\downarrow p_e + 2\gamma_0 p_0^e + \Gamma p_0^e - 2\sum_{m=0}^\infty \gamma_m^\uparrow p_0^e,
\end{aligned} \tag{E1a}$$

where γ_m describe the incoherent spontaneous emission progress $|e;0\rangle \to |g;m\rangle$ satisfying $\sum_{m=0}^{\infty}\gamma_m = \gamma$. It is obvious that the total population on the state $|e\rangle$ is the sum of all the occupations of its sublevels as $p_e = \sum_{m=0}^{\infty} p_m^e$. Thus, we have

$$\dot{p}_e = 2\sum_{m=0}^{\infty}\gamma_m^{\uparrow}p_0^g - 2\gamma p_0^e - 2\sum_{m=0}^{\infty}\gamma_m^{\downarrow}p_0^e. \tag{E2}$$

Considering less population on states $|e;m_e>0\rangle$ and $|g;m_g>0\rangle$ due to the large vibrational relaxation Γ, we can simplify Eq. (E2) into

$$\dot{p}_e = 2\sum_{m=0}^{\infty}\gamma_m^{\uparrow}(1-p_e) - 2\left(\gamma + \sum_{m=0}^{\infty}\gamma_m^{\downarrow}\right)p_e \tag{E3}$$

by assuming $p_e \approx p_0^e$ and $p_g = 1 - p_e \approx p_0^g$.

APPENDIX F: ABSORPTION AND EMISSION SPECTRA

1. Effective quantum Langevin equation for the commutator

In this subsection, we will describe the process to find the absorption and emission spectroscopic signal. Before that, let us introduce the following correlators dressed by a vibrational mode

$$\tilde{C}_{\rm em}^{e}(t+\tau) = \sigma^{\dagger}(t)\sigma(t+\tau)\mathcal{S}_e^{\dagger}(t+\tau)\mathcal{D}_e^{\dagger}(t+\tau) \quad \text{and}$$
$$\tilde{C}_{\rm em}^{g}(t+\tau) = \mathcal{S}_g^{\dagger}(t+\tau)\mathcal{D}_g^{\dagger}(t+\tau)\sigma^{\dagger}(t)\sigma(t+\tau) \tag{F1}$$

for emission and

$$\tilde{C}_{\rm ab}^{e}(t+\tau) = \sigma(t+\tau)\sigma^{\dagger}(t)\mathcal{S}_e^{\dagger}(t+\tau)\mathcal{D}_e^{\dagger}(t+\tau) \quad \text{and}$$
$$\tilde{C}_{\rm ab}^{g}(t+\tau) = \mathcal{S}_g^{\dagger}(t+\tau)\mathcal{D}_g^{\dagger}(t+\tau)\sigma(t+\tau)\sigma^{\dagger}(t) \tag{F2}$$

for absorption. According to the discussion in Appendix B, one will obtain

$$\frac{d\tilde{C}_{\rm em}^{e}}{d\tau} \approx -(i\omega_{00}+\gamma)\tilde{C}_{\rm em}^{e} - i(\nu_e-\nu_g)\tilde{C}_{\rm em}^{e}b_e^{\dagger}b_e(t+\tau) - \eta_\ell e^{-i\omega t}\sigma^{\dagger}(t)\mathcal{S}_e^{\dagger}(t+\tau)\mathcal{D}_e^{\dagger}(t+\tau)\mathcal{P}_e(t+\tau)$$
$$+\sqrt{2\gamma}\sigma^{\dagger}(t)\sigma_{\rm in}(t+\tau)\mathcal{S}_e^{\dagger}(t+\tau)\mathcal{D}_e^{\dagger}(t+\tau)\mathcal{P}_e(t+\tau), \tag{F3a}$$

$$\frac{d\tilde{C}_{\rm em}^{g}}{d\tau} \approx -(i\omega_{00}+\gamma)\tilde{C}_{\rm em}^{g} - i(\nu_e-\nu_g)b_g^{\dagger}b_g(t+\tau)\tilde{C}_{\rm em}^{e} + \eta_\ell e^{-i\omega t}\mathcal{S}_g^{\dagger}(t+\tau)\mathcal{D}_g^{\dagger}(t+\tau)\mathcal{P}_g(t+\tau)\sigma^{\dagger}(t)$$
$$+\sqrt{2\gamma}\mathcal{S}_g^{\dagger}(t+\tau)\mathcal{D}_g^{\dagger}(t+\tau)\mathcal{P}_e(t+\tau)\sigma^{\dagger}(t)\sigma_{\rm in}(t+\tau), \tag{F3b}$$

$$\frac{d\tilde{C}_{\rm ab}^{e}}{d\tau} \approx -(i\omega_{00}+\gamma)\tilde{C}_{\rm ab}^{e} - i(\nu_e-\nu_g)\tilde{C}_{\rm ab}^{e}b_e^{\dagger}b_e(t+\tau) - \eta_\ell e^{-i\omega t}\sigma^{\dagger}(t)\mathcal{S}_e^{\dagger}(t+\tau)\mathcal{D}_e^{\dagger}(t+\tau)\mathcal{P}_e(t+\tau)$$
$$+\sqrt{2\gamma}\sigma_{\rm in}(t+\tau)\sigma^{\dagger}(t)\mathcal{S}_e^{\dagger}(t+\tau)\mathcal{D}_e^{\dagger}(t+\tau)\mathcal{P}_e(t+\tau), \tag{F3c}$$

$$\frac{d\tilde{C}_{\rm ab}^{g}}{d\tau} \approx -(i\omega_{00}+\gamma)\tilde{C}_{\rm ab}^{g} - i(\nu_e-\nu_g)b_g^{\dagger}b_g(t+\tau)\tilde{C}_{\rm ab}^{e} + \eta_\ell e^{-i\omega t}\mathcal{S}_g^{\dagger}(t+\tau)\mathcal{D}_g^{\dagger}(t+\tau)\mathcal{P}_g(t+\tau)\sigma^{\dagger}(t)$$
$$+\sqrt{2\gamma}\mathcal{S}_g^{\dagger}(t+\tau)\mathcal{D}_g^{\dagger}(t+\tau)\mathcal{P}_e(t+\tau)\sigma_{\rm in}(t+\tau)\sigma^{\dagger}(t). \tag{F3d}$$

2. Emission spectra in the transient regime

We now assume the molecule is initially prepared in the excited state $|e;\tilde{0}\rangle$ to compute the spectrum of emission in the transient regime. By setting $\eta_\ell = 0$, one can obtain the expression of the two-time correlation function $\langle\sigma^{\dagger}(0)\sigma(\tau)\rangle$ through Eq. (F3):

$$\langle\sigma^{\dagger}(0)\sigma(t)\rangle = \mathcal{F}_{\rm em}(\nu_g,\tau)e^{-(i\omega_{00}+\gamma)t}. \tag{F4}$$

Taking the Fourier transformation gives the expression of the emission spectrum:

$$S_{\rm em}(\omega) = 2\mathcal{R}\int_0^{\infty} d\tau\,\mathcal{F}_{\rm em}(\nu_g,\tau)e^{[i\omega-(i\omega_{00}+\gamma)]\tau} = \sum_{m=0}^{\infty}\frac{S_m^{\rm em}(\gamma+m\Gamma)}{(\gamma+m\Gamma)^2+(\omega_{00}-\omega-m\nu_g)^2}. \tag{F5}$$

3. Absorption spectra in the stability regime

The formal solution of the two-time correlation function $\langle\sigma(t+\tau)\sigma^{\dagger}(t)\rangle$ is given by

$$\langle\sigma(t+\tau)\sigma^{\dagger}(t)\rangle = -\eta_\ell\int_t^{\infty} d\tau\,\mathcal{G}_{\rm em}(-\nu_g,t+\tau-\tau)\langle\mathcal{P}_e(\tau)\sigma^{\dagger}(t)\rangle + \eta_\ell\int_t^{\infty} d\tau\mathcal{G}_{\rm ab}(\nu_e,t+\tau-\tau)\langle\mathcal{P}_g(\tau)\sigma^{\dagger}(t)\rangle$$
$$+\mathcal{P}_g(t)\mathcal{F}_{\rm ab}(\nu_e,\tau)e^{-(i\omega_{00}+\gamma)t}. \tag{F6}$$

For simplicity, let us assume the amplitude for the driving field is very weak, so that few molecules are occupying their excited state, i.e., $\mathcal{P}_e(t) \ll 1$ and $\mathcal{P}_g(t) \approx 1$. The solution will become

$$\begin{aligned}\langle\sigma(t+\tau)\sigma^\dagger(t)\rangle &\approx \eta_\ell \int_t^\infty d\tau\, \mathcal{G}_{\rm ab}(\nu_e, t+\tau-\tau)\langle\sigma^\dagger(t)\rangle + \mathcal{F}_{\rm ab}(\nu_e,\tau)e^{-(i\omega_{00}+\gamma)\tau}\\ &= \eta_\ell \int_t^\infty d\tau\, e^{-(i\omega_{00}-i\omega_\ell+\gamma)(t+\tau-\tau)}\mathcal{F}_{\rm ab}(\nu_e, t+\tau-\tau)\Theta(t+\tau-\tau)\langle\sigma^\dagger(t)\rangle + \mathcal{F}_{\rm ab}(\nu_e,\tau)e^{-(i\omega_{00}+\gamma)\tau}. \end{aligned} \tag{F7}$$

Let us pay attention to the steady-state regime by setting $t \to \infty$. According to Eq. (D9b), we can get the expectation value of the transition dipole moment beyond the rotating frame:

$$\lim_{t\to\infty}\langle\sigma(t)\rangle = \chi_\alpha e^{-i\omega_\ell t}. \tag{F8}$$

Inserting the expression of the function $\mathcal{F}_{\rm ab}(\nu,t)$ given by Eq. (C14) into Eq. (F7), we obtain

$$\lim_{t\to\infty}\langle\sigma(t+\tau)\sigma^\dagger(t)\rangle \approx \sum_{m,n=0}^{\infty}\frac{\eta_\ell^2 S_m^{\rm ab}S_n^{\rm ab}[e^{-i\omega_\ell\tau} - e^{-(i\omega_{00}+im\nu_e+\gamma+m\Gamma)\tau}]}{[\gamma+m\Gamma+i(\omega_{00}+m\nu-\omega_\ell)][\gamma+n\Gamma-i(\omega_{00}+n\nu_e-\omega_\ell)]} \tag{F9a}$$

$$+\sum_{m=0}^{\infty} S_m^{\rm ab}e^{-(i\omega_{00}+im\nu_e+\gamma+m\Gamma)\tau}. \tag{F9b}$$

As $\eta_\ell \ll \gamma$, the contribution of the term in Eq. (F9a) can be ignored. Finally, we can simplify the expression of $\langle\sigma(t+\tau)\sigma^\dagger(t)\rangle$ into

$$\lim_{t\to\infty}\langle\sigma(t+\tau)\sigma^\dagger(t)\rangle = \sum_{m=0}^{\infty} S_m^{\rm ab}e^{-(i\omega_{00}-im\nu_e+\gamma+m\Gamma)\tau}. \tag{F10}$$

Performing the Fourier transform, the absorption spectrum is obtained as

$$S_{\rm ab}(\omega) = 2\mathcal{R}\int_0^\infty d\tau \lim_{t\to\infty}\langle\sigma(t+\tau)\sigma^\dagger(t)\rangle e^{i\omega\tau} = \sum_{m=0}^{\infty}\frac{S_m^{\rm ab}(\gamma+m\Gamma)}{(\gamma+m\Gamma)^2+(\omega+m\nu_e-\omega_{00})^2}. \tag{F11}$$

APPENDIX G: INFLUENCE OF THE ANHARMONIC TERMS

Let us introduce nonlinear terms in the Hamiltonian $\mathcal{H}_{\rm anh} = \mathcal{H}^g_{\rm anh} + \mathcal{H}^e_{\rm anh}$ to investigate the dynamics of the system beyond the harmonic approximation. We defined $\mathcal{H}^Q_{\rm anh} = \delta_Q b^\dagger b^\dagger b b \mathcal{P}_Q$ where Q stands for either g or e. Consequently, the evolution of the molecule under the classical driving will be dictated by the following Hamiltonian in the polaron picture:

$$\mathcal{H}' = \tilde{\mathcal{H}} + \mathcal{H}_{\rm anh} + i\eta_\ell(\sigma^\dagger\mathcal{S}^\dagger\mathcal{D}^\dagger e^{-i\omega_\ell t} - \sigma\mathcal{D}\mathcal{S}e^{i\omega_\ell t}). \tag{G1}$$

1. Vibrational dynamics

According to Appendix B, the Langevin equations for the vibrational mode read

$$\dot{b}_Q \approx -(i\nu_Q+\Gamma)b_Q - i2\delta_Q b_Q^\dagger b_Q b_Q + \text{noise}, \tag{G2a}$$

$$\partial_t b_Q^\dagger b_Q b_Q \approx -(i\nu_Q+2\delta_Q+3\Gamma)b_Q^\dagger b_Q b_Q + 2\delta_Q b_Q^\dagger b_Q^\dagger b_Q b_Q + \text{noise}. \tag{G2b}$$

We focus on the low occupancy limit, which should be valid for either low temperatures or high vibrational frequencies. Thus, the term $b_Q^\dagger b_Q^\dagger b_Q b_Q$ can be neglected as its average value tends to zero. Finally we have

$$\partial_t b_Q^\dagger b_Q b_Q \approx -(i\nu_Q+2\delta_Q+3\Gamma)b_Q^\dagger b_Q b_Q + \text{noise}. \tag{G2c}$$

Making use the quantum regression theorem, it is straightforward to obtain the two-time correlation function for the vibrational mode:

$$\langle b_Q(t)b_Q^\dagger(\tau)\rangle_{\rm vib} = e^{-(i\nu_Q+\Gamma)(t-\tau)}\mathcal{P}_Q. \tag{G3}$$

2. Electronic transition

We can now derive equations of motion for both polaron operators,

$$\dot{\tilde{\delta}}_e \approx -[i(\omega_{00}-\omega_\ell)+\gamma]\tilde{\delta}_e - i(\delta_e-\delta_g)\tilde{\delta}_e b_e^\dagger b_e^\dagger b_e - i(\nu_e-\nu_g)\tilde{\delta}_e b_e^\dagger b_e^\dagger b_e - \eta_\ell\mathcal{S}_e^\dagger\mathcal{D}_e^\dagger\sigma^\dagger\sigma + \sqrt{2\gamma}\sigma_{\rm in}\mathcal{S}_e^\dagger\mathcal{D}_e^\dagger, \tag{G4a}$$

$$\dot{\tilde{\delta}}_g \approx -[i(\omega_{00}-\omega_\ell)+\gamma]\tilde{\delta}_g + i(\delta_e-\delta_g)b_g^\dagger b_g^\dagger b_g\tilde{\delta}_g + i(\nu_e-\nu_g)b_g^\dagger b_g\tilde{\delta}_g + \eta_\ell\mathcal{S}_g^\dagger\mathcal{D}_g^\dagger\sigma\sigma^\dagger + \sqrt{2\gamma}\sigma_{\rm in}\mathcal{S}_g^\dagger\mathcal{D}_g^\dagger, \tag{G4b}$$

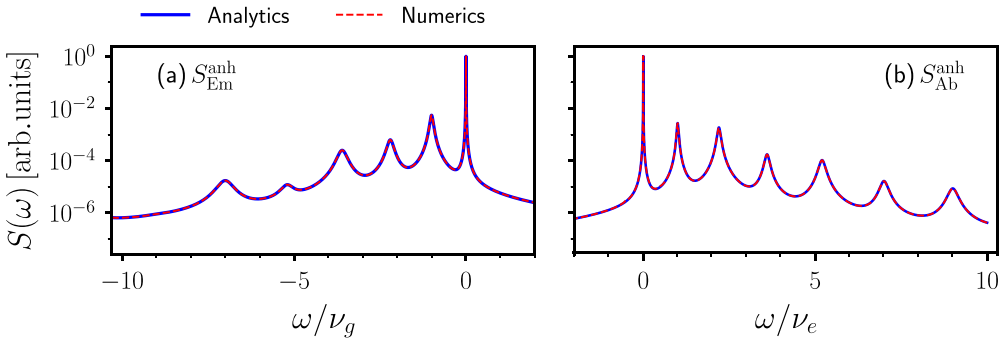

FIG. 8. Molecular spectra for (a) emission progress and (b) absorption progress. The red-dashed lines are numerical simulation under the following parameters under the following parameters $\delta_g/\nu_g = \delta_e/\nu_e = 0.1$. The others are the same as those in Fig. 3.

and formally integrate to obtain the time evolution:

$$\langle\sigma(t)\rangle = -\eta_\ell \int_0^t d\tau\, e^{-[i(\omega_{00}-\omega_\ell)+\gamma](t-\tau)} \langle \mathcal{S}_e^\dagger(\tau)\mathcal{D}_e^\dagger(\tau) e^{i(\nu_e-\nu_g)b_e^\dagger b_e \tau} e^{i(\delta_e-\delta_g)b_e^\dagger b_e^\dagger b_e b_e \tau} e^{-i(\delta_e-\delta_g)b_e^\dagger b_e^\dagger b_e b_e t} e^{-i(\nu_e-\nu_g)b_e^\dagger b_e t} \mathcal{D}_e(t)\mathcal{S}_e(t)\rangle_{\rm vib}$$
$$+ \eta_\ell \int_0^t d\tau\, e^{-[i(\omega_{00}-\omega_\ell)+\gamma](t-\tau)} \langle \mathcal{D}_g(t)\mathcal{S}_g(t) e^{-i(\nu_e-\nu_g)b_g^\dagger b_g t} e^{-i(\delta_e-\delta_g)b_g^\dagger b_g^\dagger b_g b_g t} e^{i(\delta_e-\delta_g)b_g^\dagger b_g^\dagger b_g b_g \tau} e^{i(\nu_e-\nu_g)b_g^\dagger b_g \tau} \mathcal{S}_g^\dagger(\tau))\mathcal{D}_g^\dagger(\tau)\rangle_{\rm vib}. \tag{G5}$$

Let us direct our focus to the two-time correlation function in the above expression. It is an exceedingly challenging task to obtain their expression according to the process introduced in Appendix C. Nevertheless, we can still utilize the pump-probe scenario for analysis. Since the Fock states $|m_Q\rangle$ still remain eigenstates of the anharmonic Hamiltonian $\mathcal{H}_{\rm anh}$, we can obtain the molecular transition frequencies $\omega_{00} + m\nu_e + (m^2 - m)\delta_e$ for the absorption process $|g;0_g\rangle \to |e;m_e\rangle$ and $\omega_{00} - m\nu_g - (m^2 - m)\delta_g$ for the emission progress $|e;0_e\rangle \to |g;m_g\rangle$. Consequently, we can straightforwardly derive the expressions for the correlation functions:

$$\langle \mathcal{S}_e^\dagger(0)\mathcal{D}_e^\dagger(0) e^{-i(\delta_e-\delta_g)b_e^\dagger b_e^\dagger b_e b_e t} e^{-i(\nu_e-\nu_g)b_e^\dagger b_e t} \mathcal{D}_e(t)\mathcal{S}_e(t)\rangle = \sum_{m=0}^{\infty} S_m^{\rm em} e^{[im\nu_g + i(m^2-m)\delta_g - m\Gamma]t}, \tag{G6}$$

$$\langle \mathcal{D}_g(t)\mathcal{S}_g(t) e^{-i(\nu_e-\nu_g)b_g^\dagger b_g t} e^{-i(\delta_e-\delta_g)b_g^\dagger b_g^\dagger b_g b_g t} \mathcal{S}_g^\dagger(0)\mathcal{D}_g^\dagger(0)\rangle = \sum_{m=0}^{\infty} S_m^{\rm ab} e^{-[im\nu_e + i(m^2-m)\delta_e + m\Gamma]t}. \tag{G7}$$

Correspondingly, we can obtain the molecular absorption and emission spectra:

$$S_{\rm ab}^{\rm anh}(\omega) = \sum_{m=0}^{\infty} \frac{S_m^{\rm ab}(\gamma + m\Gamma)}{(\gamma + m\Gamma)^2 + [\omega + m\nu_e + (m^2 - m)\delta_e - \omega_{00}]^2}, \tag{G8}$$

$$S_{\rm em}^{\rm anh}(\omega) = \sum_{m=0}^{\infty} \frac{S_m^{\rm em}(\gamma + m\Gamma)}{(\gamma + m\Gamma)^2 + [\omega_{00} - \omega - m\nu_g - (m^2 - m)\delta_g]^2}. \tag{G9}$$

The comparison of analytical and numerical results of the profile for the emission and absorption processes in Fig. 8 shows indeed the validity of the analytical expressions.

[1] T. Neuman and J. Aizpurua, Origin of the asymmetric light emission from molecular exciton polaritons, Optica **5**, 1247 (2018).

[2] H. J. Clark and T. J. Dines, Resonance Raman spectroscopy, and its application to inorganic chemistry, Angew. Chem. Int. Ed. Engl. **25**, 131 (1986).

[3] E. Smith and G. Dent, Chapter 4: Resonance Raman scattering, in *Modern Raman Spectroscopy: A Practical Approach* (Wiley, New York, 2005).

[4] M. Riede, B. Lüssem, K. Leo, and A. Z. M. S. Rahman, Organic semiconductors, in *Reference Module in Materials Science and Materials Engineering* (Elsevier, Amsterdam, 2018).

[5] T. Holstein, Studies of polaron motion: Part I. The molecular-crystal model, Ann. Phys. **8**, 325 (1959).

[6] F. C. Spano, Excitons in conjugated oligomer aggregates, films, and crystals, Annu. Rev. Phys. Chem. **57**, 217 (2006).

[7] M. Reitz, C. Sommer, and C. Genes, Langevin approach to quantum optics with molecules, Phys. Rev. Lett. **122**, 203602 (2019).

[8] M. Reitz, C. Sommer, B. Gurlek, V. Sandoghdar, D. Martin-Cano, and C. Genes, Molecule-photon interactions in phononic environments, Phys. Rev. Res. **2**, 033270 (2020).

[9] Z. Zhang, X. Nie, D. Lei, and S. Mukamel, Multidimensional coherent spectroscopy of molecular polaritons:

Langevin approach, Phys. Rev. Lett. **130**, 103001 (2023).
[10] Q. Zhang and K. Zhang, Collective effects of organic molecules based on the Holstein-Tavis-Cummings model, J. Phys. B **54**, 145101 (2021).
[11] K. S. U. Kansanen, J. J. Toppari, and T. T. Heikkilä, Polariton response in the presence of Brownian dissipation from molecular vibrations, J. Chem. Phys. **154**, 044108 (2021).
[12] K. S. U. Kansanen, A. Asikainen, J. J. Toppari, G. Groenhof, and T. T. Heikkilä, Theory for the stationary polariton response in the presence of vibrations, Phys. Rev. B **100**, 245426 (2019).
[13] J. Keeling and S. Kéna-Cohen, Bose–Einstein condensation of exciton-polaritons in organic microcavities, Annu. Rev. Phys. Chem. **71**, 435 (2020).
[14] J. Gilmore and R. H. McKenzie, Spin boson models for quantum decoherence of electronic excitations of biomolecules and quantum dots in a solvent, J. Phys.: Condens. Matter **17**, 1735 (2005).
[15] *Cavity Optomechanics: Nano- and Micromechanical Resonators Interacting with Light*, 1st ed., edited by M. Aspelmeyer, T. J. Kippenberg, and F. Marquardt, Quantum Science and Technology (Springer-Verlag, Berlin, 2014).
[16] M. Aspelmeyer, T. J. Kippenberg, and F. Marquardt, Cavity optomechanics, Rev. Mod. Phys. **86**, 1391 (2014).
[17] P. Rabl, Photon blockade effect in optomechanical systems, Phys. Rev. Lett. **107**, 063601 (2011).
[18] A. Nunnenkamp, K. Børkje, and S. M. Girvin, Single-photon optomechanics, Phys. Rev. Lett. **107**, 063602 (2011).
[19] S. J. Jang, Partially polaron-transformed quantum master equation for exciton and charge transport dynamics, J. Chem. Phys. **157**, 104107 (2022).
[20] J.-Q. Liao and F. Nori, Photon blockade in quadratically coupled optomechanical systems, Phys. Rev. A **88**, 023853 (2013).
[21] V. May and K. Oliver, *Charge and Energy Transfer Dynamics in Molecular Systems*, 3rd ed. (Wiley, New York, 2011).
[22] F. Herrera and F. C. Spano, Dark vibronic polaritons and the spectroscopy of organic microcavities, Phys. Rev. Lett. **118**, 223601 (2017).
[23] N. Wu, J. Feist, and F. J. Garcia-Vidal, When polarons meet polaritons: Exciton-vibration interactions in organic molecules strongly coupled to confined light fields, Phys. Rev. B **94**, 195409 (2016).
[24] H. Mustroph, J. Mistol, B. Senns, D. Keil, M. Findeisen, and L. Hennig, Relationship between the molecular structure of merocyanine dyes and the vibrational fine structure of their electronic absorption spectra, Angew. Chem. Int. Ed. **48**, 8773 (2009).
[25] R. Miao, Y. Fu, D. Lu, F. Liang, H. Yu, H. Zhang, and Y. Wu, Deciphering the vibronic lasing performances in an electron-phonon-photon coupling system, Opt. Express **31**, 9790 (2023).
[26] J. Zirkelbach *et al.*, High-resolution vibronic spectroscopy of a single molecule embedded in a crystal, J. Chem. Phys. **156**, 104301 (2022).
[27] C. Gardiner and P. Zoller, *Quantum Noise: A Handbook of Markovian and Non-Markovian Quantum Stochastic Methods with Applications to Quantum Optics* (Springer, New York, 2004).
[28] J. C. del Valle and J. Catalán, Kasha's rule: A reappraisal, Phys. Chem. Chem. Phys. **21**, 10061 (2019).
[29] A. Chenu, S.-Y. Shiau, and M. Combescot, Two-level system coupled to phonons: Full analytical solution, Phys. Rev. B **99**, 014302 (2019).
[30] S. Banerjee and G. Gangopadhyay, Spectra of displaced distorted oscillator molecular system, Chem. Phys. Lett. **359**, 295 (2002).
[31] H. J. Carmichael, *Statistical Methods in Quantum Optics 1: Master Equations and Fokker-Planck Equations*, 1st ed., Theoretical and Mathematical Physics (Springer-Verlag, Berlin, 1999).
[32] J. del Pino, F. A. Y. N. Schröder, A. W. Chin, J. Feist, and F. J. Garcia-Vidal, Tensor network simulation of non-Markovian dynamics in organic polaritons, Phys. Rev. Lett. **121**, 227401 (2018).
[33] A. Strashko, P. Kirton, and J. Keeling, Organic polariton lasing and the weak to strong coupling crossover, Phys. Rev. Lett. **121**, 193601 (2018).
[34] M. A. Sentef, M. Ruggenthaler, and A. Rubio, Cavity quantum-electrodynamical polaritonically enhanced electron-phonon coupling and its influence on superconductivity, Sci. Adv. **4**, eaau6969 (2018).
[35] F. Herrera and J. Owrutsky, Molecular polaritons for controlling chemistry with quantum optics, J. Chem. Phys. **152**, 100902 (2020).
[36] M. A. Zeb, P. G. Kirton, and J. Keeling, Exact states and spectra of vibrationally dressed polaritons, ACS Photonics **5**, 249 (2018).
[37] M. Du, L. A. Martinez-Martinez, R. F. Ribeiro, Z. Hu, V. M. Menon, and J. Yuen-Zhou, Theory for polariton-assisted remote energy transfer, Chem. Sci. **9**, 6659 (2018).
[38] R. F. Ribeiro, L. A. Martínez-Martínez, M. Du, J. Campos-Gonzalez-Angulo, and J. Yuen-Zhou, Polariton chemistry: Controlling molecular dynamics with optical cavities, Chem. Sci. **9**, 6325 (2018).
[39] D. Plankensteiner, C. Sommer, M. Reitz, H. Ritsch, and C. Genes, Enhanced collective Purcell effect of coupled quantum emitter systems, Phys. Rev. A **99**, 043843 (2019).
[40] R. F. Ribeiro, A. D. Dunkelberger, B. Xiang, W. Xiong, B. S. Simpkins, J. C. Owrutsky, and J. Yuen-Zhou, Theory for nonlinear spectroscopy of vibrational polaritons, J. Phys. Chem. Lett. **9**, 3766 (2018).
[41] R. F. Ribeiro, J. A. Campos-Gonzalez-Angulo, N. C. Giebink, W. Xiong, and J. Yuen-Zhou, Enhanced optical nonlinearities under collective strong light-matter coupling, Phys. Rev. A **103**, 063111 (2021).
[42] D. Wang, H. Kelkar, D. Martin-Cano, T. Utikal, S. Götzinger, and V. Sandoghdar, Coherent coupling of a single molecule to a scanning Fabry-Perot microcavity, Phys. Rev. X **7**, 021014 (2017).
[43] B. Gurlek, V. Sandoghdar, and D. Martin-Cano, Engineering long-lived vibrational states for an organic molecule, Phys. Rev. Lett. **127**, 123603 (2021).
[44] J. Johansson, P. Nation, and F. Nori, QuTiP: An open-source PYTHON framework for the dynamics of open quantum systems, Comput. Phys. Commun. **183**, 1760 (2012).